

OPTIMISATION OF STOCHASTIC NETWORKS WITH BLOCKING: A FUNCTIONAL-FORM APPROACH

B. PATCH, M. S. SQUILLANTE, P. M. VAN DE VEN

ABSTRACT. Many stochastic networks encountered in practice exhibit some kind of blocking behaviour, where traffic is lost due to congestion. Examples include call dropping in cellular networks, difficulties with task migration in mobile cloud computing, and depleted stock points in spare parts supply chains. Blocking can be mitigated by increasing service capacity at congested stations, but purchasing these additional resources may be costly. Thus, finding the right resource allocation requires striking a careful balance between blocking and costs, a problem which is further complicated by the stochastic nature of the network. Although certain classes of queueing networks have product-form stationary distributions that could be used to formulate the relevant optimisation problem in closed form, such results only exist for highly stylised networks, and in particular do not allow for blocking. Another class of current solution methods is simulation-based optimisation, where the resource allocation is evaluated and updated using simulation. Although this works well for small instances, the associated computational costs are prohibitive for networks of real-life size.

In this paper we propose a hybrid functional-form based approach that combines the strengths of the analytical and simulation-based approaches into a novel iterative algorithm. We do this by locally approximating the objective function through a functional form calibrated using simulation. In each iteration step we choose a new resource allocation based on this local approximation, which in turn gives rise to a new approximation. We implement this algorithm for a range of functional forms, computationally determine which work best, and provide an alternative formulation of the algorithm that does not rely on numerical solvers. Extensive computational experiments show that at similar performance levels, our functional-form approach has significantly lower computational costs compared to stochastic approximation.

KEYWORDS. simulation optimisation ◦ loss queues ◦ resource allocation ◦ stochastic approximation

AFFILIATIONS. B. Patch was with the School of Mathematics and Physics, The University of Queensland, St. Lucia, Australia and Korteweg-de Vries Institute, University of Amsterdam, The Netherlands, he is now with Centrum Wiskunde & Informatica (CWI), Netherlands (brendan@cwi.nl); M. S. Squillante is with Mathematical Sciences Department, IBM Research, United States (mss@us.ibm.com); and P. M. van de Ven is with Centrum Wiskunde & Informatica (CWI), Netherlands (ven@cwi.nl). The research for this paper is partly funded by the NWO Gravitation Programme NETWORKS, Grant Number 024.002.003 (Patch), the ARC Centre of Excellence for Mathematical and Statistical Frontiers (Patch), and an Australian Government Research Training Program (RTP) scholarship (Patch).

1. Introduction

Stochastic networks encountered in practice often involve blocking, where customers can be delayed or lost due to various forms of congestion. A key design decision for such networks concerns the allocation of resources to limit blocking while maintaining low costs.

For example, consider cellular wireless networks in which calls are handed over between cell towers as users move and calls are dropped if the receiving tower has insufficient available capacity. Naturally, call dropping should be avoided, leading to extensive study of capacity management in cellular networks

(see, e.g., [2, 36, 25]). A similar issue plays a role in mobile cloud computing, where computational jobs are served at small “cloudlets” close to the user, rather than at a remote cloud computing facility (see, e.g., [26]). While this can reduce delays, each cloudlet has limited capacity and migrating jobs between cloudlets due to user mobility may lead to job losses and, in turn, corresponding performance issues.

Another example concerns a supply chain network designed for maintaining capital goods with uncertain lifetimes. Any downtime of these goods is expensive and disruptive, and should be minimised to the extent possible. When a capital good breaks down, the necessary spare parts are quickly dispatched from the nearest stock point. If a spare part is unavailable at this location, blocking occurs and the parts must be sent from a more distant central warehouse, thus increasing downtime. According to [1], sales and services related to spare parts accounted for 8% of the gross domestic product of the United States in 2003. Consequently significant research has focused on the design of spare-parts networks to balance swift response to breakdowns with costs of maintaining a large supply of spare parts (see, e.g., [35, 24, 31]). A similar problem arises in the context of emergency services, where ambulances and fire trucks should be located to ensure a fast response to emergencies (see, e.g., [7, 38, 37]).

In the context of both types of examples above, the problem is often summarised as an optimisation problem $\max_{\mathbf{c} \in \mathcal{C}} f(\mathbf{c})$, where $f(\mathbf{c}) := \mathbb{E} F(\mathbf{c})$ is a function $\mathcal{C} \rightarrow \mathbb{R}$ from a set of parameters to be optimised to the real numbers representing a performance metric of interest. Here $F(\mathbf{c})$ is a random variable (r.v.) that follows a different law depending on the parameter \mathbf{c} . Let \mathbf{c}^* denote a solution to this optimisation problem. While this problem is often intractable for many real-world systems of practical interest, the design of such systems requires finding a parameter choice $\hat{\mathbf{c}}^*$ that ensures $f(\hat{\mathbf{c}}^*)$ is as close to $f(\mathbf{c}^*)$ as possible. Roughly speaking, there are two categories of existing approaches for solving capacity management problems in stochastic networks: analytical and simulation based.

Analytical approaches typically approximate the complex stochastic network with a much simpler network and solve the corresponding optimisation problem: $\max_{\mathbf{c} \in \mathcal{C}} \tilde{f}(\mathbf{c})$. Examples include approximations based on product-form networks (see, e.g., [5, 21, 14]), assumptions that network components behave independently (see, e.g., [4, 32]), fluid-limit scalings (see, e.g., [15]), and large-scale systems (see, e.g., [6, 16]). These closed-form approximations can then be used to solve the capacity management problem, either analytically (see, e.g., [23, 39]), numerically, or using a combination of both (see, e.g., [34]).

Simulation-based approaches typically evaluate and update capacity allocation using simulation of the stochastic network. This assumes it is possible to obtain samples $\hat{f}(\mathbf{c})$ of the r.v.s $F(\mathbf{c})$ evaluated at specific parameters \mathbf{c} , which are equal to $f(\mathbf{c})$ in expectation, and to generate a sequence of samples $(\hat{f}(\mathbf{c}^{(n)}))_{n \in \{1, \dots, N\}}$. Based on these samples, algorithms aim to solve the optimisation problem $\max_{\mathbf{c} \in \mathcal{C}} f(\mathbf{c})$, with the goals of providing rigorous performance guarantees that $\mathbf{c}^{(N)} \rightarrow \mathbf{c}^*$ as $N \rightarrow \infty$ and ensuring this convergence occurs as fast as possible (i.e., $\mathbf{c}^{(N)}$ as close to \mathbf{c}^* as possible for N as small as possible).

One canonical simulation-based optimisation approach is stochastic approximation (see, e.g., [18, 3]) in which the sequence of approximate optimisers is generated according to $\mathbf{c}^{(n+1)} = \mathbf{c}^{(n)} + \alpha^{(n)} H^{(n)} \nabla \hat{f}(\mathbf{c}^{(n)})$, with step-size $\alpha^{(n)}$, linear map $H^{(n)}$, and estimate $\nabla \hat{f}(\mathbf{c}^{(n)})$ of the Jacobian $\nabla f(\mathbf{c}^{(n)})$. When $H^{(n)}$ is an identity matrix and $\alpha^{(n)} = \beta/n$, for some $\beta \in \mathbb{R}^+$, we recover the classical algorithm of [33]. Meanwhile, when $H^{(n)}$ is an identity matrix and $\nabla \hat{f}(\mathbf{c}^{(n)})$ is estimated using finite differences, we recover the classical algorithm of [22]; in this case, $\sum_{n=1}^{\infty} \alpha^{(n)} = \infty$ and other conditions on the sequence of finite difference estimates must hold for convergence to be guaranteed. These algorithms represent adaptations of gradient descent to the stochastic setting. Such adaptations of Newton and quasi-Newton type methods,

where $H^{(n)}$ is taken to be the inverse of the Hessian matrix, is currently a very active area of research (see, e.g., [9]).

Both analytical and simulation approaches have limitations that prevent straightforward application to the complex stochastic networks of interest. In analytical approaches, it is often impossible to find an approximation for the complex network that is sufficiently accurate and captures all relevant features; as a result, any capacity management decisions based on the approximate model may not work well in the original model. Simulation-based approaches display better accuracy, but can suffer from large computational costs, which often make their application to high-dimensional complex stochastic networks infeasible.

Recently, [12] introduced a hybrid approach that exploits theoretical properties of the stochastic network to significantly reduce the computational costs of the simulation-based approach. Simulation is exploited to evaluate the (unknown in closed form) performance metric f subject to noise at particular capacity choices according to a r.v. $\hat{f}(\mathbf{c})$ with $\mathbb{E} \hat{f}(\mathbf{c}) = f(\mathbf{c})$. Analytical methods are exploited to approximate f by a functional form \tilde{f} based on theoretical properties of the network and to directly optimise \tilde{f} . The combination forms an iteration process comprising, for every iteration n , the simulation of $\hat{f}(\mathbf{c}^{(n)})$ to obtain parameters of \tilde{f} such that (s.t.) $\tilde{f}(\mathbf{c}^{(n)}) = \hat{f}(\mathbf{c}^{(n)})$ and the setting of $\mathbf{c}^{(n+1)} = \arg \max_{\mathbf{c} \in \mathcal{C}} \tilde{f}(\mathbf{c})$. The authors show that, for this generated sequence with a well chosen functional form \tilde{f} , $\mathbf{c}^{(n)} \rightarrow \hat{\mathbf{c}}$ where $\hat{\mathbf{c}}$ is close to \mathbf{c}^* . Starting from $\hat{\mathbf{c}}$, stochastic approximation is then used to obtain a final optimal solution \mathbf{c}^* . [12] show that such a hybrid approach works exceptionally well for the stochastic networks without blocking of interest therein, notably not requiring estimates of the Jacobian or Hessian.

The specific approach of [12], however, does not easily carry over to our setting herein, where the addition of blocking fundamentally changes the dynamics of the stochastic network. Moreover, the objective function changes from a function of the queue lengths to one of the blocking probabilities, together with the additional complexity of discrete capacities for the number of servers at each station of the network rather than per-station service rates. In this paper we devise a functional-form approach to optimise stochastic networks with blocking by extending the basic approach of [12], as well as proposing and evaluating the performance of several potential functional forms. We apply our approach to realistic examples, evaluate the method using standard and non-standard networks, and show that it can outperform stochastic approximation.

The remainder of this paper is organised as follows. Section 2 provides an overview of our functional-form optimisation approach, followed by a presentation our stochastic network model and the relevant objective function. Section 4 describes our search for a good functional form, and then we consider modifying this form to circumvent the need for a numerical solver. Section 6 demonstrates that these algorithms work well on a realistic network under a variety of scenarios, followed by concluding remarks in Section 7.

2. Overview of Functional-Form Approach

The objective of our study is to determine parameters \mathbf{c} , from a set of possible network parameters \mathcal{C} , that maximise a function $f : \mathcal{C} \rightarrow \mathbb{R}$ representing a performance metric of interest. Here, $\mathbf{c} \in \mathcal{C}$ could parametrise the service rate or number of servers at each station of a stochastic network, and $f(\mathbf{c})$ could capture features of the transient or steady-state behaviour of the network. In this paper we consider \mathbf{c} to be the number of servers and $f(\mathbf{c})$ to be the rate in equilibrium at which customers depart from the

system without entering service (fraction of blocked customers). Note that [12] consider $f(\mathbf{c})$ to be the weighted expected number of customers in the system in equilibrium.

A primary difficulty in determining the value

$$\mathbf{c}^* := \arg \max_{\mathbf{c} \in \mathcal{C}} f(\mathbf{c}) \quad (1)$$

comes from the fact that the function f is typically unknown, owing to the complexity of our stochastic network, and therefore we assume it can only be evaluated as a r.v. F s.t. $\mathbb{E} F(\mathbf{c}) = f(\mathbf{c})$. With time-consuming simulation, it is possible to obtain samples of F , denoted by \hat{f} , and use the information contained in these samples to find an approximation of \mathbf{c}^* . The objective of this paper is to develop a method for closely approximating \mathbf{c}^* using as few evaluations of F as possible, for a specific model detailed in the next section.

The functional-form optimisation approach exploits underlying theoretical properties of f to augment information from simulation and speed up the iteration process of finding a good approximation to \mathbf{c}^* . This structural information is expressed as a closed-form function $\tilde{f}(\mathbf{c}, \boldsymbol{\tau})$ of both the network parameters \mathbf{c} and some additional (potentially vector-valued) parameters $\boldsymbol{\tau}$, and used to tune \tilde{f} so that it fits f well locally. Depending on the complexity of \tilde{f} we then solve, either analytically or numerically, for

$$\tilde{\mathbf{c}}^* = \arg \max_{\mathbf{c} \in \mathcal{C}} \tilde{f}(\mathbf{c}, \boldsymbol{\tau}) \quad (2)$$

to approximate \mathbf{c}^* . The function \tilde{f} is selected to ensure that (2) can be solved in closed form or using a fast numerical procedure, which is in stark contrast to solving for (1).

The quality of the approximation (2) relies in large part on choosing an \tilde{f} that properly represents fundamental behaviours of the stochastic network. We assume $\boldsymbol{\tau}$ is selected from an appropriate set s.t. the set of functions $\{\tilde{f}(\cdot, \boldsymbol{\tau})\}_{\boldsymbol{\tau}}$ has elements that approximate f well and that can be reliably identified in terms of $\boldsymbol{\tau}$. For the remainder of this section we shall assume a good functional form is known and provide an iterative procedure for choosing $\boldsymbol{\tau}$, where the sequence of samples $(\hat{f}^{(n)})_{n=1,\dots,N}$ is used to guide our selection of $\boldsymbol{\tau}$.

Starting with an initial value of $\mathbf{c} = \mathbf{c}^{(0)}$, which can be chosen in various ways (e.g., [12] use their analytical solution for the corresponding product-form network), we evaluate $\hat{f}(\mathbf{c}^{(0)})$ using simulation, set $\hat{f}(\mathbf{c}^{(0)}) = \tilde{f}(\mathbf{c}^{(0)}, \boldsymbol{\tau}^{(1)})$, and solve for $\boldsymbol{\tau}^{(1)}$. This renders our iteration 1 approximation function $\tilde{f}^{(1)}(\cdot) := \tilde{f}(\cdot, \boldsymbol{\tau}^{(1)})$, as depicted in Figure 1a¹. Then, from (2), we solve $\mathbf{c}^{(1)} := \arg \max_{\mathbf{c}} \tilde{f}^{(1)}(\mathbf{c})$ to obtain our iteration 1 approximation for \mathbf{c}^* .

Continuing in this manner, we evaluate $\hat{f}(\mathbf{c}^{(1)})$ via simulation and solve $\hat{f}(\mathbf{c}^{(1)}) = \tilde{f}(\mathbf{c}^{(1)}, \boldsymbol{\tau}^{(2)})$ for $\boldsymbol{\tau}^{(2)}$ to obtain our iteration 2 approximation $\tilde{f}^{(2)}(\cdot) := \tilde{f}(\cdot, \boldsymbol{\tau}^{(2)})$ that intersects f at $\mathbf{c} = \mathbf{c}^{(1)}$ in expectation; see Figure 1b. Observe that, while selection of the functional form \tilde{f} requires fundamental insights into the behaviours of the stochastic network, our approach does not rely solely on inaccurate queueing formulas, in contrast to purely analytic approximations, because simulation is used to evaluate the stochastic network.

In general, our iteration process consists of the sequence of approximation functions

$$\tilde{f}^{(n)}(\cdot) := \tilde{f}(\cdot, \boldsymbol{\tau}^{(n)}), \quad n = 1, 2, \dots, \quad (3)$$

¹Although the domain of f is one-dimensional in Figure 1a for ease of illustration, we are generally interested in high-dimensional stochastic networks which is a primary cause of complexity for the problems under consideration.

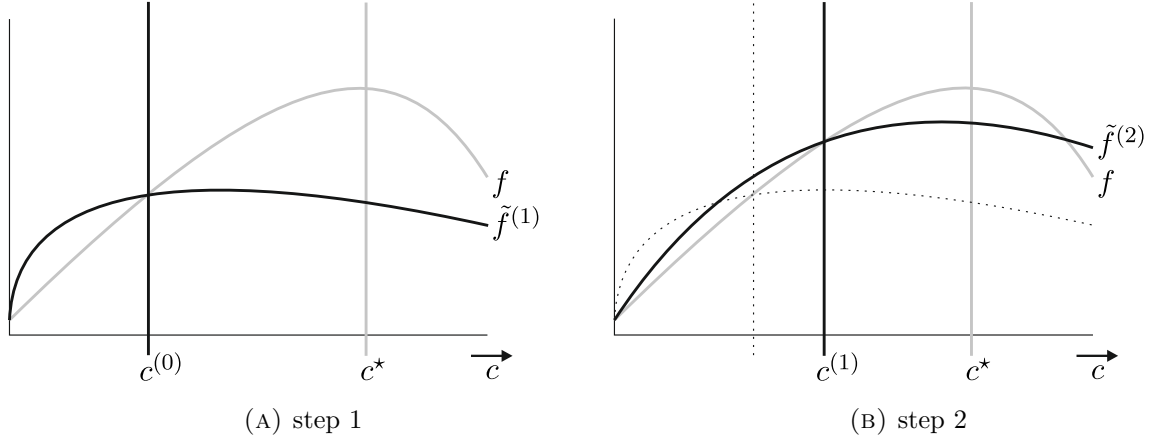


FIGURE 1. Two iteration steps of a functional-form optimisation algorithm.

with corresponding maximisers

$$\mathbf{c}^{(n)} := \arg \max_{\mathbf{c} \in \mathcal{C}} \tilde{f}^{(n)}(\mathbf{c}), \quad n = 1, 2, \dots, \quad (4)$$

where the tuning parameter $\tau^{(n)}$ in each iteration is obtained by solving

$$\hat{f}(\mathbf{c}^{(n-1)}) := \tilde{f}(\mathbf{c}^{(n-1)}, \tau^{(n)}), \quad n = 1, 2, \dots. \quad (5)$$

Assuming convergence of the process, we iterate (3) – (5) until the difference $\|\mathbf{c}^{(n)} - \mathbf{c}^{(n-1)}\|$ is sufficiently small. This approach relies on the fact that $\tilde{f}(\cdot, \tau^{(n)})$ provides a good approximation for f around $\mathbf{c} = \mathbf{c}^{(n-1)}$ and thus the algorithm is likely to move in the proper direction at each iteration. This also provides significant computational improvements over purely simulation-based methods: Instead of, for instance, running many expensive simulations to estimate the Jacobian (or Hessian) as in stochastic approximation, our functional-form approach essentially uses \tilde{f} (a function $\mathcal{C} \rightarrow \mathbb{R}$) to provide $\nabla \tilde{f}(\mathbf{c})$ as an approximation for the gradients $\nabla f(\mathbf{c})$, which requires only a single inexpensive evaluation of \hat{f} per iteration. Beyond these computational savings, we also believe that this approach is less sensitive to the variance of \hat{F} than approaches that rely on estimates of gradients (since it uses only point estimates which are likely to be less noisy than gradient estimates).

Following [12], when this approximation needs to be further refined, the final $\mathbf{c}^{(n)}$ can be used as a starting point for a simulation-based optimisation approach with guaranteed convergence properties, such as stochastic approximation. This second stage may have improved accuracy over our functional-form approach above, but it also can be computationally costly. However, by first obtaining a near-optimal solution using our fast hybrid functional-form approach, the more expensive purely simulation-based approach requires far fewer iterations to find the optimal solution, thus significantly reducing the overall computational costs over exclusively using simulation-based optimisation.

3. Stochastic Networks with Blocking

We now define the stochastic network model and the corresponding optimisation problem formulation, followed by some specific examples. It is important to note that the applicability of our general approach, and even of our eventual choice of functional form, is by no means limited to this class of models. Moreover, since the full model is only evaluated using simulation (in order to estimate $f(\mathbf{c}^{(n-1)})$) as discussed in Section 2, one may add many details and extensions to the simulation model that are not

present in the model defined below. Meanwhile, it is important to retain the basic components of this stochastic model (e.g., blocking, no waiting room) in order to obtain the best possible results.

3.1. Mathematical Model. Consider a stochastic network comprising a set of stations $\mathcal{L} := \{1, \dots, L\}$; e.g., each station could represent a base station in a cellular network or a stock point in a spare-parts network. Customers arrive to the network according to exogenous arrival processes, move between stations to receive service, and then depart from the network. Station l has c_l servers that can each serve a customer; we refer to c_l as the capacity of station l and define $\mathbf{c} := (c_l)_{l=1, \dots, L}$. When a customer arrives at a station to find no available server, it will immediately depart the network and we say the customer has been *blocked* or *lost*. However, if a station to which a customer arrives has an available server, it is accepted for service and remains at the server of the station for a generally distributed amount of time with finite expectation — we impose no other restrictions on the service distributions.

Each customer belongs to a class $r \in \mathcal{R} = \{1, \dots, R\}$ that is associated with a path comprising N_r network stations defined by $\psi_r := (l_i^{(r)})_{i=1, \dots, N_r}$, $l_i^{(r)} \in \mathcal{L}$. We assume no station appears more than once in any set ψ_r , i.e., $l_i^{(r)} \neq l_j^{(r)}$, $\forall i \neq j$, but otherwise the path is completely general. A class- r customer arrives to the system at station $l_1^{(r)} \in \mathcal{L}$. Upon completion of service at station $l_i^{(r)}$, for $i = 1, \dots, N_r - 1$, the customer transitions to station $l_{i+1}^{(r)}$ and either receives service or is blocked depending on whether a server is available at the station. The customer leaves the network after receiving service at station $l_{N_r}^{(r)}$.

Consider a stochastic optimisation problem encountered by a network operator who collects rewards for service completions and incurs costs for provisioning servers. Each server at station l costs $\theta_l > 0$ per unit time and each service completion of a class- r customer at station $l_i^{(r)}$ generates $\omega_{r,i} > 0$ rewards. Define $\boldsymbol{\theta} := (\theta_l)_{l=1, \dots, L}$ and $\boldsymbol{\omega}_r := (\omega_{r,i})_{i=1, \dots, N_r}$. If a customer is blocked at station $l_i^{(r)}$, $i > 1$, then rewards are collected for the successful service completions at the preceding stations $l_1^{(r)}, \dots, l_{i-1}^{(r)}$ and potential rewards $l_i^{(r)}, \dots, l_{N_r}^{(r)}$ are forfeited. This model seeks to address the fundamental trade-off between maintaining low capacity costs and maintaining high reward collections (by ensuring few blockages).

Let $A_{r,i}(t)$ denote the number of class- r arrivals to station $l_i^{(r)}$ in the time interval $[0, t]$, which for $i > 1$ depends on the blocking experienced by class- r customers at stations $l_1^{(r)}, \dots, l_{i-1}^{(r)}$ and the exogenous arrivals of class- r customers. The number of exogenous class- r arrivals to the network over $[0, t]$ is given by $A_{r,1}(t)$. Based on observations of arrivals and blockages for each class at each station over a long time horizon (through simulation), we determine the long-run average class- r arrival rate that we assume exists and converges with probability 1 to a deterministic constant $\lambda_r \in \mathbb{R}_+$ as time t goes to infinity:

$$\frac{1}{t} \int_0^t A_{r,1}(s) ds \rightarrow \lambda_r, \quad \text{as } t \rightarrow \infty. \quad (6)$$

No further assumptions are made on the arrival processes, allowing as examples renewal type with independent and identically distributed interarrival times (see, e.g., [8, 28]) and Markovian arrival processes with non-identically distributed interarrival times (see, e.g., [17, 27]).

Let $B_{r,i}(t)$ denote the number of class- r blockages at station $l_i^{(r)}$ in the time interval $[0, t]$. Based on observations of these blockages over very long periods of time (via simulation) in combination with our corresponding observations of arrivals, we determine the long-run proportion of class- r customers arriving at station $l_i^{(r)}$ that are subsequently blocked at the station. We assume this quantity, which depends on the capacity of the stations, converges with probability 1 to a deterministic constant $p_{r,i}(\mathbf{c}) \in (0, 1]$ as time t goes to infinity:

$$\frac{B_{r,i}(t)}{A_{r,i}(t)} \rightarrow p_{r,i}(\mathbf{c}) \quad \text{as } t \rightarrow \infty. \quad (7)$$

Define $\varpi_r := (\varpi_{r,i})_{i=1,\dots,N_r}$, $\varpi_{r,i} := \prod_{j=1}^i (1 - p_{r,j}(\mathbf{c}))$, and let $\langle \cdot, \cdot \rangle$ be the usual inner product operator. To optimise the performance of the above system operating in equilibrium, we express the corresponding expected net rate of reward generation by the system as

$$f(\mathbf{c}) = -\langle \mathbf{c}, \boldsymbol{\theta} \rangle + \sum_{r \in \mathcal{R}} \lambda_r \langle \boldsymbol{\omega}_r, \varpi_r \rangle. \quad (8)$$

This expression serves as our objective function, which is inspired by the *capacity value function* investigated by [11, 10] in the context of Erlang-B loss systems and later generalised by [29] in the context of provisioning cloud computing platforms. Our optimisation formulation seeks to determine

$$\mathbf{c}^* := \arg \max_{\mathbf{c} \in \mathbb{Z}_+^L} f(\mathbf{c}). \quad (9)$$

The capacity values above are discrete, however application of our optimisation approach will involve continuous functions of \mathbf{c} . We therefore make the following assumption.

Assumption 1. *When a customer arrives to a station with (non-integer) capacity c and finds $\lfloor c \rfloor + 1$ customers, the customer is blocked. If an arrival encounters $\lfloor c \rfloor$ customers, the newly arriving customer is accepted with probability $c - \lfloor c \rfloor$, and blocked otherwise. When an arrival finds less than or equal to $\lfloor c \rfloor - 1$ customers, the arrival is accepted.*

The above assumption results in a continuous relaxation of the objective function that matches (8) at integer points. Whenever our (approximate) optimal solution is non-integer, we round to the closest integer. In addition, we make a natural non-degeneracy assumption that the optimal capacity allocation is strictly positive. The implication of this assumption is that we are essentially working with systems that are known to be profitable with respect to (w.r.t.) naive capacity choices and the overall goal is to improve the level of profitability.

Assumption 2. *The optimal capacity is greater than or equal to one for all stations, that is $c_l^* \geq 1$ for $l = 1, \dots, L$.*

3.2. Illustrative problem instances. Our model represents stochastic networks with blocking such as cellular networks where calls can be lost (dropped) from local base stations and instead resolved by the network protocol, as well as spare-parts networks where parts can be lost (unavailable) from local stock points and instead handled by a central warehouse; our formulation represents the corresponding optimisation problems where $\boldsymbol{\theta}$ reflects the costs incurred for per-station capacities in both types of networks, $\boldsymbol{\omega}$ reflects the rewards received for servicing calls at every base station in cellular networks with lost calls causing forfeited rewards, and $\boldsymbol{\omega}$ reflects the benefits received for dispatching parts at every stock point in spare-parts networks with central warehouse delays causing forfeited benefits. The following four problem instances illustrate some of the complexities that arise in practical applications, with the last example providing a flavour of the type of systems for which our approach is intended.

Example 1. Starting with a classical telecommunications problem, consider a system with a single station, a single customer class, capacity c_1 ; see Figure 2a. Customers arrive from a Poisson process with rate λ_1 and have generally distributed service times with mean μ^{-1} . Hence, $\mathcal{L} = \{1\}$, $\psi_1 = (1)$, $l_1^{(1)} = 1$. The long-run proportion of blocked customers in this M/G/c/c queue is given by the well-known Erlang-B loss formula ([21]):

$$p_{1,1}(c_1) = \frac{(\lambda_1/\mu)^{c_1}/c_1!}{\sum_{i=0}^{c_1} (\lambda_1/\mu)^i/i!}. \quad (10)$$

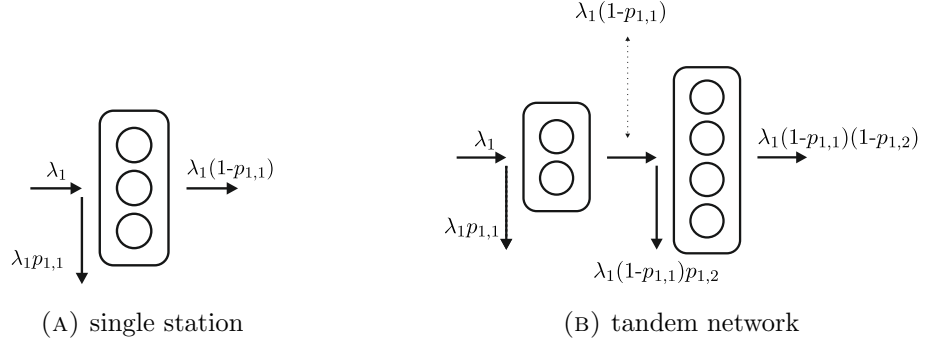


FIGURE 2. Two small network instances.

With capacity costs θ_1 per unit time to provision and rewards $\omega_{1,1}$ per successful call service completion, the objective function (8) can be explicitly evaluated over $\mathcal{C} = \mathbb{N}$ as

$$f(c_1) = -c_1 \theta_1 + \lambda_1 \omega_{1,1} (1 - p_{1,1}(c_1)). \quad (11)$$

Although not directly amenable to calculus-based optimisation due to the discrete nature of the denominator in (10), it is straightforward to evaluate this function on modern computers and the optimal capacity can be found by brute force for relatively large c_1 .

Example 2. Now consider the above system with a second customer classes. Class r customers arrive from a Poisson process with rate λ_r and, upon successful service at the station, depart the system. Hence, $\mathcal{L} = \{1\}$, $\mathcal{R} = \{1, 2\}$, $\psi_1 = (1)$, $l_1^{(1)} = 1$, $\psi_2 = (1)$, $l_1^{(2)} = 1$. With capacity costs θ_1 per unit time to provision and rewards $\omega_{1,1}$ and $\omega_{2,1}$ per successful class 1 and 2 service completion, we maximise over $\mathcal{C} = \mathbb{N}^2$ the objective function given by

$$f(\mathbf{c}) = -\theta_1 c_1 + \lambda_1 \omega_{1,1} (1 - p_{1,1}(c_1)) + \lambda_2 \omega_{2,1} (1 - p_{2,1}(c_1)). \quad (12)$$

Example 3. Next consider a system with two stations, a single customer class, and capacities c_1, c_2 ; see Figure 2b. Customers arrive to station 1 from a Poisson process with rate λ_1 and, upon successful service at station 1, attempt service at station 2. Hence, $\mathcal{L} = \{1, 2\}$, $\mathcal{R} = \{1\}$, $\psi_1 = (1, 2)$, $l_1^{(1)} = 1$, $l_2^{(1)} = 2$. Observe that, while $p_{1,1}(c_1)$ is independent of c_2 , $p_{1,2}(\mathbf{c})$ depends on both c_1 and c_2 because larger c_1 renders a larger number of arrivals to station 2. With capacity costs θ_1 and θ_2 per unit time to provision and rewards $\omega_{1,1}$ and $\omega_{1,2}$ per successful service completion at stations 1 and 2, respectively, the objective function (8) is given by

$$f(\mathbf{c}) = -\theta_1 c_1 - \theta_2 c_2 + \lambda_1 \omega_{1,1} (1 - p_{1,1}(c_1)) + \lambda_1 \omega_{1,2} (1 - p_{1,1}(c_1)) (1 - p_{1,2}(\mathbf{c})), \quad (13)$$

which is maximised over $\mathcal{C} = \mathbb{N}^2$. We provide in Appendix A an explicit expression for $f(\mathbf{c})$ that we exploit in Section 5.2 to evaluate the performance of our general approach.

Example 4. Lastly, consider a six-station, twelve-class system, $\mathbf{c} = (c_1, \dots, c_6)$, $\mathcal{L} = \{1, \dots, 6\}$, $\mathcal{R} = \{1, \dots, 12\}$, where the customer classes follow the network paths $\psi_1 = (1)$, $\psi_2 = (1, 3)$, $\psi_3 = (1, 3, 5)$, $\psi_4 = (1, 4)$, $\psi_5 = (1, 4, 5)$, $\psi_6 = (1, 4, 6)$, $\psi_7 = (2)$, $\psi_8 = (2, 4)$, $\psi_9 = (2, 4, 6)$, $\psi_{10} = (2, 3)$, $\psi_{11} = (2, 3, 6)$, $\psi_{12} = (2, 3, 5)$. Customers of each class arrive to the first per-path station according to a per-class renewal process and have a different per-station service time that is the same for all classes. In Section 6 we apply our general approach to this system with capacity costs θ_l per unit time to provision station l s.t. $|\boldsymbol{\theta}| = 6$ and rewards $\omega_{r,l}$ per successful service completion of class- r customers at station l s.t. $|\boldsymbol{\omega}| = 28$.

4. Finding Appropriate Functional Form

Now consider our functional-form approach to solve the resource optimisation problem (9), recalling we cannot directly solve (9) because the objective function (8) must be evaluated via simulation. A functional form tailored to the specific model of interest can have significant benefits over existing frameworks that assume a generic objective function, such as stochastic approximation. We first discuss the simplest case to identify good functional-form candidates, and then we extend this approach to the case of general networks.

4.1. Simple case. For the single-station, single-class network in **Example 1** of Section 3.2, and depicted in Figure 2a, the problem formulation consists of determining the server capacity $c_1 \in \mathbb{N}$ that maximises the objective function (11). Here the costs θ_1 and rewards $\omega_{1,1}$ are known constants, and the arrival rate λ_1 is independent of the capacity and assumed to be known (alternatively, it can be found from simulation). The blocking probability $p_{1,1}(c_1)$, however, depends on the long-term behaviour of the underlying stochastic process and is not explicitly known in general; the exception, of course, is the case of Poisson arrivals where $p_{1,1}$ is given by (10).

Since $p_{1,1}$ contains all complex aspects of $f(\cdot)$, with the remainder of f only serving to connect the intricate reward-reducing blocking behaviour in the system, we need a function $\tilde{p}_{1,1}(\cdot, \tau_{1,1})$ that well approximates $p_{1,1}$ in order to identify a functional-form approximation

$$\tilde{f}(c_1, \tau_{1,1}) = -c_1 \theta_1 + \lambda_1 \omega_{1,1} (1 - \tilde{p}_{1,1}(c_1, \tau_{1,1})). \quad (14)$$

Given an appropriate choice for $\tilde{p}_{1,1}$, our Algorithm 1 implements the iterative algorithm (3) – (5) for a desired level of accuracy $\epsilon > 0$ and a maximum number of steps $N \in \mathbb{N}$.

Algorithm 1: Single-station optimisation

Result: Approximation to optimal capacity allocation.

```

1 Choose  $c_1^{(0)} > 0$ ,  $\epsilon > 0$ ,  $N \in \mathbb{N}$ ;
2 Set  $n = 1$  and  $g > \epsilon$ ;
3 while  $g > \epsilon$  and  $n \leq N$  do
4   Evaluate  $\hat{p}_{1,1}(c_1^{(n-1)})$  using simulation;
5   Solve for  $\tau_{1,1}^{(n)}$  in  $\hat{p}_{1,1}(c_1^{(n-1)}) = \tilde{p}_{1,1}(c_1^{(n-1)}, \tau_{1,1}^{(n)})$ ;
6   As an approximation to the optimal capacity, set  $c_1^{(n)} = \arg \max_{c_1 > 0} -c_1 \theta_1 + \lambda_1 \omega_{1,1} (1 - \tilde{p}_{1,1}(c_1, \tau_{1,1}^{(n)}))$ ;
7   Set  $g = \|c_1^{(n-1)} - c_1^{(n)}\|$  and  $n = n + 1$ ;
8 end
9 Output  $c_1^{(n)}$ .

```

Some key desirable properties for an appropriate functional form include: (i) behaviour similar to the blocking probability in a corresponding loss system as a function of c_1 ; (ii) $\tilde{p}_{1,1}$ convex and decreasing in c_1 so that the blocking probability decreases as the capacity increases; (iii) $\tilde{p}_{1,1}(0, \cdot) = 1$, i.e., always block if there is no capacity; (iv) $\lim_{c \rightarrow \infty} \tilde{p}_{1,1}(c, \cdot) = 0$, i.e., the blocking probability goes to 0 as the capacity grows large; (v) unique $\tau_{1,1}$ -solution to Step 5 of Algorithm 1, for all $c_1 \geq 0$; and (vi) $\tilde{p}_{1,1}$ analytically differentiable in c_1 with an identified solution so that numerical solutions of Step 6 in Algorithm 1 are not necessary.

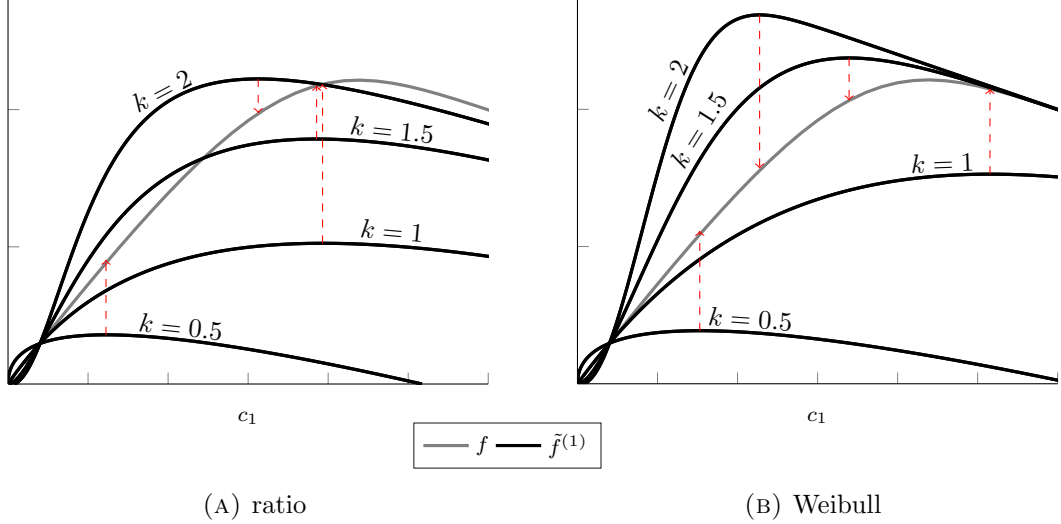


FIGURE 3. Approximations of the ratio and Weibull functional forms with $k = 0.5, 1, 1.5, 2$.

Although a substantial literature exists on the analysis of the Erlang-B formula (10) (see, e.g., [19, 13, 30, 20]), functional forms inspired by these works do not meet the desirable properties (v) and (vi) and lead to poor approximations. Instead, after extensive computational exploration of a variety of forms, we selected two far simpler expressions that showed promise: the ratio form

$$\tilde{p}_{1,1}(c_1, \tau_{1,1}) = \left(1 + (\tau_{1,1} c_1)^k\right)^{-1}, \quad (15)$$

and the Weibull form

$$\tilde{p}_{1,1}(c_1, \tau_{1,1}) = \exp\left(-(c_1)^k\right). \quad (16)$$

Note that both expressions contain an additional variable $k \geq 0$ that can be fine-tuned, thus inducing a family of functional forms for each. Our primary source of inspiration for these functional forms was related to cumulative probability distribution functions for r.v.s with non-negative support. Some such forms were immediately discarded because of their complexity; for example, the gamma and log-normal distribution functions were eliminated due to the presence of factorials and error functions. We performed the computations presented later in this section for a variety of different forms (i.e., Pareto, trapezoidal, reciprocal), finding that (15) and (16) showed the most potential. We also investigated switching the role of k and $\tau_{1,1}$ in (16), but the results were not encouraging.

For both the ratio and Weibull functional forms, Step 5 of Algorithm 1 can be computed in closed form. In particular, after straightforward algebraic manipulations, we have that the solution of Step 5 in Algorithm 1 for the ratio form can be written as

$$\tau_{1,1}^{(n)} = \frac{1}{c_1^{(n-1)}} \left(\frac{1 - \hat{p}_{1,1}(c_1^{(n-1)})}{\hat{p}_{1,1}(c_1^{(n-1)})} \right)^{1/k}, \quad (17)$$

and that the corresponding solution for the Weibull form can be expressed as

$$\tau_{1,1}^{(n)} = \frac{1}{c_1^{(n-1)}} \left(-\log(\hat{p}_{1,1}(c_1^{(n-1)})) \right)^{1/k}. \quad (18)$$

In both cases, the solution to Step 6 of Algorithm 1 is then computed numerically.

To illustrate the quality of these functional forms, Figure 3 plots the objective function f (gray) and several typical approximations \tilde{f} (black) based on both ratio and Weibull forms for different values of k . We consider the representative case with $\lambda_1 = 16$, $\theta_1 = 0.2$, and $\omega_{1,1} = 1$, noting that the following

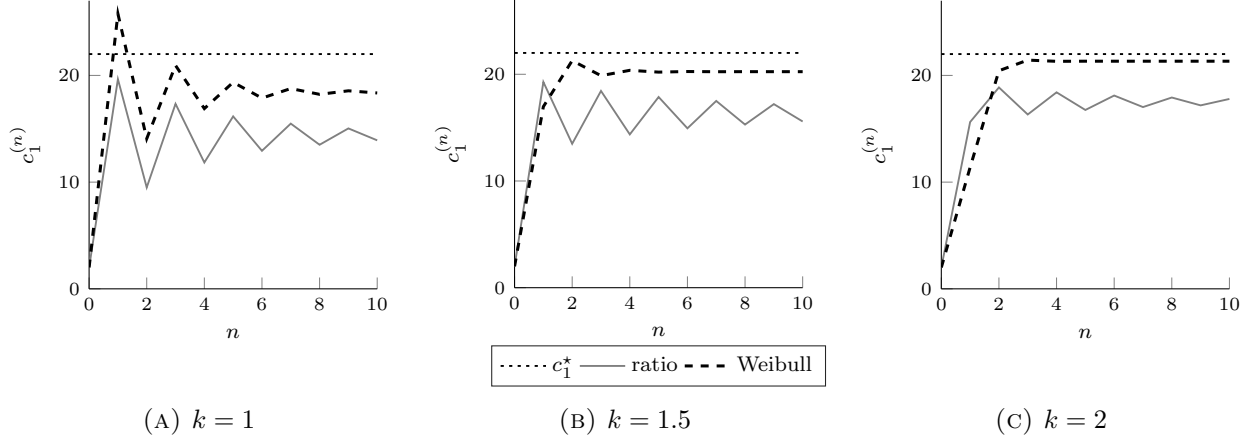
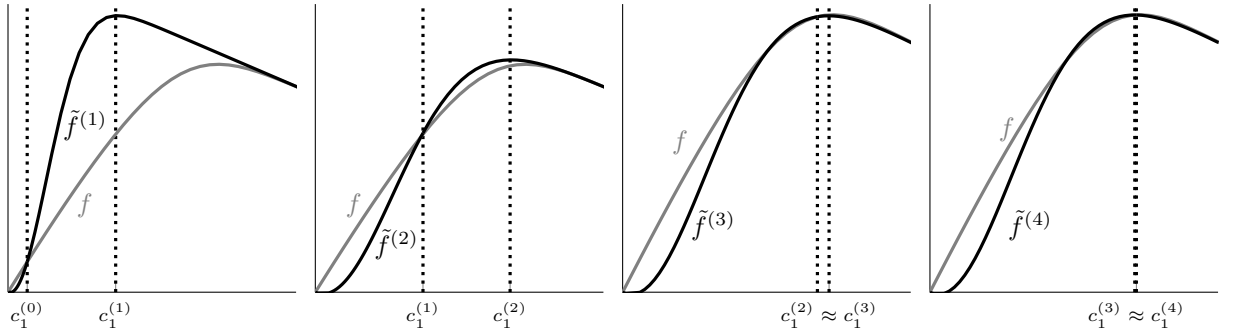


FIGURE 4. Evolution of Algorithm 1 for the ratio and Weibull functional forms.

FIGURE 5. First four iterations for the Weibull functional form with $k = 2$.

discussion holds more generally for the other parameter choices examined. Figure 3a plots $f(c_1)$ and $\tilde{f}(c_1, \tau_{1,1}^{(1)})$ from (14) with $\tilde{p}_{1,1}$ the ratio form (15) for $k = 0.5, 1, 1.5, 2$ and $\tau_{1,1}^{(1)}$ obtained from (17) with $c_1^{(0)} = 2$. Figure 3b presents the same results for the Weibull form (16) and the corresponding value of $\tau_{1,1}^{(1)}$ obtained from (18).

Inspection of these results shows that the ratio form with $k = 1.5$ or $k = 1$ provides $c_1^{(1)}$ values close to optimal, despite these functions being quite different w.r.t. how closely they track the actual value of the objective function. This highlights the importance of having an approximate function with curvature (derivative values) similar to the actual objective function near the true optimiser. For both families of functions, $k = 0.5$ performs poorly.

The results in Figure 3 represent a single iteration of Algorithm 1. Figure 4 shows how $c_1^{(n)}$ evolves for both forms with $k = 1, 1.5, 2$. Observe that the Weibull form with $k = 2$ returns the best approximate optimiser, perhaps surprisingly since it performed quite poorly in comparison to others after one iteration (see Figure 3). To further investigate this, Figure 5 plots both $f(c_1)$ and $\tilde{f}^{(n)}(c_1, \tau)$ from (14) with $\tilde{p}_{1,1}(c_1, \tau_{1,1}^{(n)})$ the Weibull form (16), $k = 2$, $n = 1, 2, 3, 4$. Namely, we compare the true objective function to the approximate objective functions obtained from the first four iterations of Algorithm 1. Clearly, by the fourth iteration, the Weibull functional form performs very well locally around the true optimiser.

4.2. General networks. To extend Algorithm 1 from the single-station, single-class case to a general network, we must approximate the blocking probability for each combination of class and per-path station with a functional form. Recall that $p_{r,i}(\mathbf{c})$ denotes the long-run proportion of class- r customers blocked at the i -th station of their path ψ_r (i.e., $l_i^{(r)}$) as a function of the resource allocation \mathbf{c} . The functional-form

approximation for $p_{r,i}(\mathbf{c})$ is then given by

$$p_{r,i}(\mathbf{c}) \approx \tilde{p}_{r,i} \left(c_{l_i^{(r)}}, \tau_{r,i} \right), \quad r \in \mathcal{R}, \quad i = 1, \dots, N_r.$$

Note that $\tilde{p}_{r,i}$ only depends on the resource allocation at station $l_i^{(r)}$. While done for simplicity, we shall see from computational experiments that this approximation works quite well.

Each (class, per-path station) pair has its own parameter $\tau_{r,i}$ that needs to be determined based on the simulated blocking probability $\hat{p}_{r,i}(\mathbf{c}^{(n-1)})$ by solving the equation

$$\hat{p}_{r,i}(\mathbf{c}) = \tilde{p}_{r,i} \left(c_{l_i^{(r)}}, \tau_{r,i} \right). \quad (19)$$

Once these $\tau_{r,i}$ are determined, we then can obtain a new approximation to the optimal resource allocation problem by evaluating the corresponding version of (8) and (9):

$$\arg \max_{\mathbf{c} \in (0, \infty)^L} -\langle \mathbf{c}, \boldsymbol{\theta} \rangle + \sum_{r \in \mathcal{R}} \lambda_r \sum_{i=1}^{N_r} \omega_{r,i} \prod_{j=1}^i \left(1 - \tilde{p}_{r,j} \left(c_{l_j^{(r)}}, \tau_{r,j} \right) \right).$$

Algorithm 2: General network optimisation

Result: Approximation to optimal capacity allocation.

- 1 Choose $\mathbf{c}^{(0)} \in (0, \infty)^L$, $\epsilon > 0$, $N \in \mathbb{N}$;
- 2 Set $n = 1$ and $g > \epsilon$;
- 3 **while** $g > \epsilon$ and $n \leq N$ **do**
- 4 For $r \in \mathcal{R}$ and $i = 1, \dots, N_r$, evaluate $\hat{p}_{r,i}(\mathbf{c}^{(n-1)})$ using simulation;
- 5 For $r \in \mathcal{R}$ and $i = 1, \dots, N_r$, solve for $\tau_{r,i}^{(n)}$ in $\hat{p}_{r,i}(\mathbf{c}^{(n-1)}) = \tilde{p}_{r,i}(c_{l_i^{(r)}}, \tau_{r,i})$;
- 6 As an approximation to the optimal capacity, solve

$$\mathbf{c}^{(n)} = \arg \max_{\mathbf{c} \in (0, \infty)^L} -\langle \mathbf{c}, \boldsymbol{\theta} \rangle + \sum_{r \in \mathcal{R}} \lambda_r \sum_{i=1}^{N_r} \omega_{r,i} \prod_{j=1}^i \left(1 - \tilde{p}_{r,j} \left(c_{l_j^{(r)}}, \tau_{r,j}^{(n)} \right) \right) \quad (20)$$

- 7 Set $g = \|\mathbf{c}^{(n-1)} - \mathbf{c}^{(n)}\|$ and $n = n + 1$;
- 8 **end**
- 9 Output $\mathbf{c}^{(n)}$.

This procedure is summarised in Algorithm 2. For the single-station, single-class case of Section 4.1, both the ratio form (15) and the Weibull form (16) perform well. Table 1 provides the corresponding extensions to general networks and to τ -solutions of (19). Note that there are two additional functional forms (c) and (d) listed in Table 1 — these form the basis for an enhancement to our approach, which is discussed in the next section.

5. Functional Form Refinements

Step 6 of Algorithm 2 requires a numerical solver for all but the simplest cases. To circumvent this, we now present various modifications to the functional forms that allow us to analytically solve Step 6. We show in Section 6 that these enhancements also improve the algorithm performance. Our presentation proceeds in four stages: Section 5.1 modifies the functional forms to eliminate the need for a numerical solver in a single-station network; Section 5.2 extends this to the case of a tandem network; Section 5.3 extends the approach to the case of a two-class network; and Section 5.4 extends our approach to general networks

TABLE 1. Functional forms and associated tuning parameters for Algorithm 2.

	Name	$\tilde{p}_{1,1}(c_1^{(n)}, \tau_{1,1}^{(n)})$	$\tau_{1,1}^{(n)}(\hat{p}_{1,1}(c_1^{(n-1)}))$
(a)	Ratio	$\left(1 + (\tau_{1,1}^{(n)} c_1^{(n)})^k\right)^{-1}$	$\frac{1}{c_1^{(n-1)}} \left(\frac{1 - \hat{p}_{1,1}(c_1^{(n-1)})}{\hat{p}_{1,1}(c_1^{(n-1)})}\right)^{1/k}$
(b)	Weibull	$\exp\left(-(\tau_{1,1}^{(n)} c_1^{(n)})^k\right)$	$\frac{1}{c_1^{(n-1)}} \left(-\log(\hat{p}_{1,1}(c_1^{(n-1)}))\right)^{1/k}$
(c)	Modified ratio	$- \int_0^{c_1^{(n)}} k c_1^{(n-1)k-1} \tau_{1,1}^{(n)k} \left(1 + (\tau_{1,1}^{(n)} x)^k\right)^{-2} dx$	$\frac{1}{c_1^{(n-1)}} \left(\frac{1 - \hat{p}_{1,1}(c_1^{(n-1)})}{\hat{p}_{1,1}(c_1^{(n-1)})}\right)^{1/k}$
(d)	Modified Weibull	$- \int_0^{c_1^{(n)}} k c_1^{(n-1)k-1} \tau_{1,1}^{(n)k} \exp\left(-(\tau_{1,1}^{(n)} x)^k\right) dx$	$\frac{1}{c_1^{(n-1)}} \left(-\log(\hat{p}_{1,1}(c_1^{(n-1)}))\right)^{1/k}$

based on the insights gained from Sections 5.1 – 5.3. Although the general case algorithm of Section 5.4 is self-contained, the preceding sections provide important intuition, justification, and motivation for our general algorithm by gradually identifying the right class of functional-form approximations and eliminating those that do not work well, starting from the simplest network and progressively adding more complexity. Each of the following subsections refers to a corresponding subsection in Appendix C, where simulation-based evidence to support the various modifications is provided.

5.1. Single-station case. Section 4.1 presented two types of functional forms for the single-station single-class case, demonstrating that they perform very well with the right parameters. The Weibull functional form with $k = 2$ was especially promising in all of the experiments we conducted. This section enhances the functional forms from Section 4.1 to allow for an analytical solution of Step 6 in Algorithm 1, while retaining their good performance.

Step 6 of Algorithm 1 requires us to find $c^{(n)}$ that maximises $\tilde{f}(c_1^{(n)}, \tau_{1,1}^{(n)}) = -c_1^{(n)} \theta_1 + \lambda_1 \omega_{1,1} (1 - \tilde{p}_{1,1}(c_1^{(n)}, \tau_{1,1}^{(n)}))$. Due to concavity and differentiability (and deferring consideration of boundary conditions until later), this requires analytically solving for $c_1^{(n)}$ in $d\tilde{f}(c_1^{(n)}, \tau_{1,1}^{(n)})/dc_1^{(n)} = 0$ and thus renders for the ratio form (15)

$$k c_1^{(n)k-1} \tau_{1,1}^{(n)k} \left(1 + (\tau_{1,1}^{(n)} c_1^{(n)})^k\right)^{-2} = -\frac{\theta_1}{\lambda_1 \omega_{1,1}} \quad (21)$$

and for the Weibull form (16)

$$k c_1^{(n)k-1} \tau_{1,1}^{(n)k} \exp\left(-(\tau_{1,1}^{(n)} c_1^{(n)})^k\right) = -\frac{\theta_1}{\lambda_1 \omega_{1,1}}. \quad (22)$$

To illustrate why solving (21) and (22) is analytically intractable in general, consider the Weibull functional form with $k = 2$, in which case (22) reduces to

$$c_1^{(n)} \exp\left(-(\tau_{1,1}^{(n)} c_1^{(n)})^2\right) = -\frac{\theta_1}{2 \tau_{1,1}^{(n)2} \lambda_1 \omega_{1,1}}. \quad (23)$$

Solving the above equation w.r.t. $c_1^{(n)}$ relies on evaluation of the *Lambert W function* that is well-known to require numerical approximation.

The key difficulty in solving (21) and (22) is the appearance of $c_1^{(n)}$ twice in each equation, as an exponential term and as a polynomial term. We therefore consider replacing one of the appearances of $c_1^{(n)}$ with $c_1^{(n-1)}$ to the solve for the former in terms of the latter. This straightforward solution turns out to be very effective, working well in all cases when we replace $c_1^{(n)}$ appearing as a polynomial term. Then, for the ratio function (21) we have

$$k c_1^{(n-1)k-1} \tau_{1,1}^{(n)k} \left(1 + (\tau_{1,1}^{(n)} c_1^{(n)})^k\right)^{-2} = \frac{\theta_1}{\lambda_1 \omega_{1,1}} \quad (24)$$

and for the Weibull function (22) we obtain

$$kc_1^{(n-1)^{k-1}}\tau_{1,1}^{(n)^k}\exp\left(-(\tau_{1,1}^{(n)}c_1^{(n)})^k\right)=\frac{\theta_1}{\lambda_1\omega_{1,1}}. \quad (25)$$

By integrating the left-hand side of (24) and (25) w.r.t. $c_1^{(n)}$, we obtain a modified ratio functional form and modified Weibull functional form, respectively. These results are summarised in Table 1, together with the functional forms from Section 4.1 for comparison. Observe that the $\tau_{1,1}^{(n)}$ results in Table 1 are identical for (c) and (a) and for (d) and (b), which is because we compute $\tau_{1,1}^{(n)}$ using $c_1^{(n-1)}$ before replacing one of the $c_1^{(n)}$ to simplify Step 6 of Algorithm 1. Further observe for these new functional forms that property (ii) above, i.e., $\tilde{p}(0) = 1$, does not necessarily hold. As previously seen in Figure 3, however, this may not be an issue as long as the curvature of \tilde{f} matches that of f around \mathbf{c}^* .

Upon solving (24) and (25) for $c_1^{(n)}$, we can explicitly replace the numerical optimisation in Step 6 of Algorithm 1 with the expressions for the ratio and Weibull modified forms

$$c_1^{(n)} = \frac{1}{\tau_{1,1}^{(n)}} \left(-1 + \sqrt{\frac{kc_1^{(n-1)^{k-1}}\tau_{1,1}^{(n)^k}\lambda_1\omega_{1,1}}{\theta_1}} \right)^{1/k} \vee 1$$

and

$$c_1^{(n)} = \frac{1}{\tau_{1,1}^{(n)}} \left(\log \left(\frac{kc_1^{(n-1)^{k-1}}\tau_{1,1}^{(n)^k}\lambda_1\omega_{1,1}}{\theta_1} \right) \right)^{1/k} \vee 1,$$

respectively, where the maximum operator is due to the boundary condition chosen to satisfy Assumption 2.

We performed extensive simulations to confirm that forms (c) and (d) perform very similarly to (a) and (b), respectively. One example is provided in Appendix C.1, where Figure 9 plots the progression of the algorithm using the modified forms (c) and (d) in comparison with the corresponding cases using (a) and (b) (with the same parameter settings as used in Figure 4, but with an initial condition $c_1^{(0)} = 30$).

5.2. Tandem networks. We expand our exploration to include the tandem-station, single-class network in **Example 3** of Section 3.2, depicted in Figure 2b. Based on the objective function (13) for this model, we aim to find the optimal capacity allocation (c_1, c_2) . The costs θ_1, θ_2 and rewards $\omega_{1,2}, \omega_{1,1}$ are known constants, and the arrival rate λ_1 is known or can be found from simulation. As in the single-station single-class case, we need to approximate the blocking proportions $p_{1,1}$ and $p_{1,2}$ with functions $\tilde{p}_{1,1}$ and $\tilde{p}_{1,2}$ to find a good functional form

$$\tilde{f}(\mathbf{c}, \boldsymbol{\tau}) = -\theta_1 c_1 - \theta_2 c_2 + \lambda_1 \omega_{1,1} (1 - \tilde{p}_{1,1}(c_1, \tau_{1,1})) + \lambda_1 \omega_{1,2} (1 - \tilde{p}_{1,1}(c_1, \tau_1)) (1 - \tilde{p}_{1,2}(c_2, \tau_{1,2})). \quad (26)$$

In this case we compute the iteration process (3) – (5) as described in Algorithm 2 where (20) is given more explicitly by (26).

While this algorithm could be implemented using either of the functional-forms (a) and (b) in Table 1 and numerically solving Step 6, we seek a closed-form solution to Step 6. To do so, we evaluate (26) at $(c_1^{(n)}, c_2^{(n)})$ and differentiate, yielding the set of equations

$$\frac{\partial}{\partial c_1^{(n)}} \tilde{f}(\mathbf{c}^{(n)}, \boldsymbol{\tau}^{(n)}) = -\theta_1 - \frac{d\tilde{p}_{1,1}(c_1^{(n)}, \tau_{1,1}^{(n)})}{dc_1^{(n)}} \left(\lambda_1 \omega_{1,1} + \lambda_1 \omega_{1,2} (1 - \tilde{p}_{1,2}(c_2^{(n)}, \tau_{1,2}^{(n)})) \right), \quad (27)$$

$$\frac{\partial}{\partial c_2^{(n)}} \tilde{f}(\mathbf{c}^{(n)}, \boldsymbol{\tau}^{(n)}) = -\theta_2 - \frac{d\tilde{p}_{1,2}(c_2^{(n)}, \tau_{1,2}^{(n)})}{dc_2^{(n)}} \left(\lambda_1 \omega_{1,2} (1 - \tilde{p}_{1,1}(c_1^{(n)}, \tau_{1,1}^{(n)})) \right). \quad (28)$$

Setting (27) and (28) equal to 0 renders a system of equations that we want to solve in order to obtain a next approximation for the optimal capacity allocation.

We saw in the previous subsection that, when $c_1^{(n)}$ appears multiple times in an equation to be solved for an optimal value (e.g., (23)), replacing all but one appearance of $c_1^{(n)}$ with $c_1^{(n-1)}$ yields a highly simplified equation that can be solved in closed form. However, doing so for (27) and (28) renders equations that contain both $c_1^{(n)}$ and $c_2^{(n)}$, still requiring highly intricate manipulations to solve. We instead decouple the solutions for $c_1^{(n)}$ and $c_2^{(n)}$: replace all appearances of $c_2^{(n)}$ with $c_2^{(n-1)}$ in (27) and all appearances of $c_1^{(n)}$ with $c_1^{(n-1)}$ in (28). To this end, let \tilde{f}_l denote the use of \tilde{f} to optimise capacity at station l . Consequently, we work with the set of functions $\{\tilde{f}_1, \tilde{f}_2\}$ in place of \tilde{f} , thus implicitly defining \tilde{f}_1 and \tilde{f}_2 as

$$\frac{\partial}{\partial c_1^{(n)}} \tilde{f}_1(c_1^{(n)}, \tau_1^{(n)}) = -\theta_1 - \frac{d\tilde{p}_{1,1}(c_1^{(n)}, \tau_1^{(n)})}{dc_1^{(n)}} \left(\lambda_1 \omega_{1,1} + \lambda_1 \omega_{2,1} (1 - \hat{p}_{1,2}(\mathbf{c}^{(n-1)})) \right), \quad (29)$$

$$\frac{\partial}{\partial c_2^{(n)}} \tilde{f}_2(c_2^{(n)}, \tau_2^{(n)}) = -\theta_2 - \frac{d\tilde{p}_{1,2}(c_2^{(n)}, \tau_2^{(n)})}{dc_2^{(n)}} \left(\lambda_1 \omega_{2,1} (1 - \hat{p}_{1,1}(\mathbf{c}^{(n-1)})) \right). \quad (30)$$

For example, under a modified Weibull form with $k = 2$ (introduced in (25)), we have

$$\begin{aligned} \frac{\partial}{\partial c_1^{(n)}} \tilde{f}_1(c_1^{(n)}, \tau_1^{(n)}) &= -\theta_1 + 2c_1^{(n-1)}\tau_1^{(n)2} \exp\left(-(\tau_1^{(n)}c_1^{(n)})^2\right) \left(\lambda_1 \omega_1 + \lambda_1 \omega_2 (1 - \hat{p}_{1,2}(\mathbf{c}^{(n-1)})) \right), \\ \frac{\partial}{\partial c_2^{(n)}} \tilde{f}_2(c_2^{(n)}, \tau_2^{(n)}) &= -\theta_2 + 2c_2^{(n-1)}\tau_2^{(n)2} \exp\left(-(\tau_2^{(n)}c_2^{(n)})^2\right) \left(\lambda_1 \omega_2 (1 - \hat{p}_{1,1}(\mathbf{c}^{(n-1)})) \right). \end{aligned}$$

Setting these to 0 and solving allows us to derive explicit expressions for $c_1^{(n)}$ and $c_2^{(n)}$:

$$c_1^{(n)} = \frac{1}{\tau_1^{(n)}} \sqrt{\log\left(\frac{2\lambda_1 c_1^{(n-1)} \tau_1^{(n)2} [\omega_1 + \omega_2 (1 - \hat{p}_{1,2}(\mathbf{c}^{(n-1)}))] }{\theta_1}\right)} \vee 1, \quad (31)$$

$$c_2^{(n)} = \frac{1}{\tau_2^{(n)}} \sqrt{\log\left(\frac{2\lambda_2 c_2^{(n-1)} \tau_2^{(n)2} \omega_2 (1 - \hat{p}_{1,1}(\mathbf{c}^{(n-1)})) }{\theta_2}\right)} \vee 1. \quad (32)$$

This yields the additional functional-form options (c) and (d) in Table 1, each of which can be varied according to a parameter k . While the functional forms (a) and (b) in Table 1 can be used in Algorithm 2 with a numerical solver, the functional form (d) can be used to directly obtain (31) and (32) for Step 6 of Algorithm 2; and the functional form (c) can be used in a similar fashion. We consider these results more generally in Section 5.

For the simple tandem network herein, it is possible to explicitly evaluate the objective function (13) using matrix analytic methods (MAMs). Although this approach does not extend to more complex settings, we present these derivations in Appendix A to enable an exact evaluation of the various functional forms, which we detail in Appendix C.2. Our key finding, as elaborated on in Appendix C.2, is that the modified functional forms for tandem networks, which do not require a numerical optimisation solver, appear to exhibit comparable accuracy and efficiency to the originally proposed forms.

5.3. Two customer classes. Considering **Example 2** from Section 3.2, we next return to the single station case but with an additional class of customers. The objective function in this case is given by (12) which can be approximated by replacing the blocking proportions $p_{1,r}$ with any functional form $\tilde{p}_{1,r}$,

such as those listed in Table 1, leading to

$$\tilde{f}(\mathbf{c}, \boldsymbol{\tau}) = -\theta_1 c_1 + \lambda_1 \omega_{1,1} (1 - \tilde{p}_{1,1}(c_1, \tau_{1,1})) + \lambda_2 \omega_{2,1} (1 - \tilde{p}_{2,1}(c_1, \tau_{2,1})). \quad (33)$$

Adapting the statement of Algorithm 2 to this model is straightforward: in Steps 4 and 5 replace $p_{1,2}$ and $\tilde{p}_{1,2}$ with $p_{2,1}$ and $\tilde{p}_{2,1}$ respectively, and in Step 6 use (33) instead of (26).

Seeking a closed-form solution to Step 6, we differentiate \tilde{f} from (33) w.r.t. $c_1^{(n)}$ to obtain

$$\frac{\partial}{\partial c_1^{(n)}} \tilde{f}(\mathbf{c}^{(n)}, \boldsymbol{\tau}^{(n)}) = -\theta_1 - \frac{d\tilde{p}_{1,1}(c_1^{(n)}, \tau_{1,1}^{(n)})}{dc_1^{(n)}} \lambda_1 \omega_{1,1} - \frac{d\tilde{p}_{2,1}(c_1^{(n)}, \tau_{2,1}^{(n)})}{dc_1^{(n)}} \lambda_2 \omega_{2,1}. \quad (34)$$

Setting this equation equal to 0, we observe that it cannot be solved in closed form and it contains multiple instances of $c_1^{(n)}$, for all functional forms (a) – (d). We overcame this difficulty in Section 5.2 by replacing all but one of the appearances of $c_1^{(n)}$ with $c_1^{(n-1)}$. Since $c_1^{(n)}$ plays a fundamentally different role in the second and third terms on the right hand side of (34), it is less clear which appearance to replace with $c_1^{(n-1)}$.

Our approach consists of combining $\tilde{p}_{1,1}(c_1^{(n)}, \tau_{1,1}^{(n)})$ and $\tilde{p}_{2,1}(c_1^{(n)}, \tau_{2,1}^{(n)})$ into a single function $\tilde{p}_1(c_1^{(n)}, \tau_1^{(n)})$, and then replacing $\tilde{p}_{1,1}(c_1^{(n)}, \tau_{1,1}^{(n)})$ and $\tilde{p}_{2,1}(c_1^{(n)}, \tau_{2,1}^{(n)})$ with $w_{1,1} \tilde{p}_1(c_1^{(n)}, \tau_1)$ and $w_{2,1} \tilde{p}_1(c_1^{(n)}, \tau_1)$, respectively, where $w_{1,1}$ and $w_{2,1}$ are appropriately chosen weights (as explained below). This results in the following functional form

$$f(\mathbf{c}, \tau_1^{(n)}) = -\theta_1 c_1 + [\lambda_1 \omega_{1,1} (1 - w_{1,1} \tilde{p}_1(c_1, \tau_1^{(n)})) + \lambda_2 \omega_{2,1} (1 - w_{2,1} \tilde{p}_1(c_1, \tau_1^{(n)}))], \quad (35)$$

which is only fully specified given a procedure for choosing the weights $w_{1,1}$ and $w_{2,1}$ and the function \tilde{p}_1 . We now cover the details of such a procedure.

Recall $A_{r,i}(t)$ as the number of class r customer arrivals to the i -th station of the class- r path in the interval $[0, t]$, and $B_{r,i}(t)$ the number of class r customers blocked from entry to this station in $[0, t]$. Once again, observing sample paths of these processes allows us to estimate $p_{r,i}(\mathbf{c})$. Letting $n_{l,r}$ denote the index of station $l_i^{(r)}$, i.e., $n_{l,r} = i$ for station $l_i^{(r)}$, we define $A_l(t) := \sum_{r:l \in r} A_{r,n_{l,r}}(t)$ to be the total number of customers arriving at station l in $[0, t]$, and similarly define $B_l(t) := \sum_{r:l \in r} B_{r,n_{l,r}}(t)$ to be the total number of customers blocked at station l in $[0, t]$. Following our approach leading to (7), we define $p_l(\mathbf{c})$ to be the almost sure limit of the proportion of customers blocked at station l :

$$\frac{B_l(t)}{A_l(t)} \rightarrow p_l(\mathbf{c}), \quad \text{as } t \rightarrow \infty, \quad (36)$$

which is the long-run proportion of customers blocked at station l (assuming existence). Note that estimates $\hat{p}_l(\mathbf{c})$ for $p_l(\mathbf{c})$ can be generated at the same time as estimates $\hat{p}_{r,i}(\mathbf{c})$ with almost no additional computational burden. The weight $w_{r,i}$ given to $\tilde{p}_{r,i}$ when replaced with $\tilde{p}_{l_i^{(r)}}$ in (35) is then defined in terms of $\hat{p}_{l_i^{(r)}}$ as

$$w_{r,i} := \frac{\hat{p}_{r,i}(\mathbf{c})}{\hat{p}_{l_i^{(r)}}(\mathbf{c})},$$

which is exact if the per-class arrival processes are independent Poisson processes.

Next, we want to consider \tilde{p}_1 utilising the functional forms in Table 1. For example, in the Weibull case with $k = 2$, $\tilde{p}_1(c_1, \tau_1^{(n)}) = \exp(-(c_1 \tau_1^{(n)})^2)$ where τ_1 is found by solving $\hat{p}_l(\mathbf{c}) = \tilde{p}_l(c_1, \tau_1^{(n)})$. Then we can evaluate (35) at $c_1^{(n)}$ and differentiate to obtain

$$\frac{\partial}{\partial c_1^{(n)}} \tilde{f}(c_1^{(n)}, \tau_1^{(n)}) = -\theta_1 - \frac{d\tilde{p}_1(c_1^{(n)}, \tau_1^{(n)})}{dc_1^{(n)}} [\lambda_1 \omega_{1,1} w_{1,1} + \lambda_2 \omega_{2,1} w_{2,1}].$$

For our modified forms (c) and (d), the above expression can be explicitly evaluated. Upon letting $\gamma_1 = \lambda_1\omega_{1,1}w_{1,1} + \lambda_2\omega_{2,1}w_{2,1}$, this renders for the modified ratio form

$$c_1^{(n)} = \frac{1}{\tau_1^{(n)}} \left(-1 + \sqrt{\frac{\gamma_1 k c_1^{(n-1)k-1} \tau_1^{(n)k}}{\theta_1}} \right)^{1/k} \vee 1,$$

and for the modified Weibull form

$$c_1^{(n)} = \frac{1}{\tau_1^{(n)}} \left(\log \left(\frac{\gamma_1 k c_1^{(n-1)k-1} \tau_1^{(n)k}}{\theta_1} \right) \right)^{1/k} \vee 1.$$

From our computational experiments for a simple network consisting of two customer classes, as presented in Appendix C.3, we continue to observe that our modified forms provide comparable accuracy and efficiency to the originally proposed forms.

5.4. General networks. Sections 5.1 – 5.3 introduced variations of our functional forms for small network instances, supporting analytical solutions of Step 6 in Algorithm 2. We now combine the lessons drawn from these special cases in order to devise an approach for general networks.

Recalling the per-station total blocking proportion p_l in (36), the intuition of Section 5.2 points us towards using a set of functional-form approximations $\{\tilde{f}_l\}_{l \in \mathcal{L}}$ where in iteration n of the algorithm we have a $(\tilde{f}_l^{(n)}(c_l^{(n)}), c_l^{(n)} > 0)$, for each $l \in \mathcal{L}$, with all $c_{l'}^{(n)}$ for $l' \in \mathcal{L} \setminus \{l\}$ replaced by $c_{l'}^{(n-1)}$. Note that, since we are working with forms (c) or (d), many instances of $c_l^{(n)}$ have already been replaced by $c_l^{(n-1)}$ relative to using (a) or (b). Then, incorporating the intuition of Section 5.3, we replace each remaining $\tilde{p}_{r,i}(c_l^{(n)}, \tau_{r,i}^{(n)})$ in \tilde{f}_l with $w_{r,i}\tilde{p}_l(c_l^{(n)}, \tau_l^{(n)})$ where $w_{r,i} = \frac{\hat{p}_{r,i}(\mathbf{c})}{\hat{p}_{l_i^{(r)}}(\mathbf{c})}$ and \tilde{p}_l utilises a form from Table 2. Let $1_l[\cdot] : \mathcal{L} \rightarrow \{0, 1\}$ be an indicator function which takes a station $l_i^{(r)}$ and returns 1 if $l_i^{(r)} = l$ and 0 otherwise. Similarly, let $\bar{1}_l[\cdot] : \mathcal{L} \rightarrow \{0, 1\}$ be an indicator function which takes a station $l_i^{(r)}$ and returns 1 if $l_i^{(r)} \neq l$ and 0 otherwise. This results in a collection of functional forms $\{\tilde{f}_l\}_{l \in \mathcal{L}}$ where

$$\tilde{f}_l(\mathbf{c}^{(n)}, \tau_l^{(n)}) = -\langle \mathbf{c}, \boldsymbol{\theta} \rangle + \sum_{r \in \mathcal{R}} \lambda_r \sum_{i=1}^{N_r} \omega_{r,i} \prod_{j=1}^i \left(1 - 1_l[l_j^{(r)}] w_{r,j} \tilde{p}_l(c_l^{(n)}, \tau_l^{(n)}) - \bar{1}_l[l_j^{(r)}] \hat{p}_{r,j}(\mathbf{c}^{(n-1)}) \right),$$

from which we derive

$$\frac{\partial \tilde{f}_l}{\partial c_l^{(n)}}(\mathbf{c}^{(n)}, \tau_l) = -\theta_l - \frac{d\tilde{p}_l(c_l^{(n)}, \tau_l^{(n)})}{dc_l^{(n)}} \sum_{r \in \mathcal{R}} \lambda_r \sum_{i=1}^{N_r} \omega_{r,i} \prod_{j=1}^i \left(1_l[l_j^{(r)}] w_{r,j} + \bar{1}_l[l_j^{(r)}] (1 - \hat{p}_{r,j}(\mathbf{c}^{(n-1)})) \right).$$

Setting this expression to 0 yields an alternative to numerical optimisation that can be used in Step 6 of our algorithm. This ‘per-station’ approach is summarised in Algorithm 3.

Noting that the second term in Step 6 of Algorithm 3 is just a constant, and following our handling of the modified Weibull form with $k = 2$ in (31) and (32) for the tandem network, we solve Step 6 of Algorithm 3 explicitly for the functional forms (c) and (d) as given in Table 2. This renders for the modified ratio form

$$c_l^{(n)} = \frac{1}{\tau_l^{(n)}} \left(-1 + \sqrt{\frac{\gamma_l k c_l^{(n-1)k-1} \tau_l^{(n)k}}{\theta_l}} \right)^{1/k} \vee 1, \quad (37)$$

Algorithm 3: Per-station functional-form optimisation

Result: Approximation to optimal capacity allocation.

- 1 Choose $\mathbf{c}^{(0)} \in (0, \infty)^L$, $\epsilon > 0$, $N \in \mathbb{N}$;
- 2 Set $n = 1$ and $g > \epsilon$;
- 3 **while** $g > \epsilon$ and $n \leq N$ **do**
- 4 Using simulation, evaluate $\hat{p}_{r,i}(\mathbf{c}^{(n-1)})$ for $r \in \mathcal{R}$, $i = 1, \dots, N_r$, and evaluate $\hat{p}_l(\mathbf{c}^{(n-1)})$ for $l \in \mathcal{L}$;
- 5 For $l \in \mathcal{L}$, solve for $\tau_l^{(n)}$ in $\hat{p}_l(\mathbf{c}^{(n-1)}) = \tilde{p}_l(\mathbf{c}^{(n-1)}, \tau_l)$;
- 6 As an approximation to the optimal capacity, for $l \in \mathcal{L}$ solve

$$\frac{d\tilde{p}_l(c_l^{(n)}, \tau_l^{(n)})}{dc_l} + \theta_l \left[\sum_{r \in \mathcal{R}} \lambda_r \sum_{i=1}^{N_r} \omega_{r,i} \prod_{j=1}^i (1_{l[l_j^{(r)}]} w_{r,j} + \bar{1}_l[l_j^{(r)}] (1 - \hat{p}_{r,j}(\mathbf{c}^{(n-1)}))) \right]^{-1} = 0;$$
- 7 Set $g = \|\mathbf{c}^{(n-1)} - \mathbf{c}^{(n)}\|$ and $n = n + 1$;
- 8 **end**
- 9 Output $\mathbf{c}^{(n)}$.

TABLE 2. Functional forms and associated tuning parameters for Algorithm 3.

	Name	$\tilde{p}_l(c_l^{(n)}, \tau_l^{(n)})$	$\tau_l^{(n)}(\hat{p}_l(\mathbf{c}^{(n-1)}))$
(c)	Modified ratio	$-\int_0^{c_l^{(n)}} k c_l^{(n-1)^{k-1}} \tau_l^{(n)^k} (1 + (\tau_l^{(n)} x)^k)^{-2} dx$	$\frac{1}{c_l^{(n-1)}} \left(\frac{1 - \hat{p}_l(\mathbf{c}^{(n-1)})}{\hat{p}_l(\mathbf{c}^{(n-1)})} \right)^{1/k}$
(d)	Modified Weibull	$-\int_0^{c_l^{(n)}} k c_l^{(n-1)^{k-1}} \tau_l^{(n)^k} \exp(-(\tau_l^{(n)} x)^k) dx$	$\frac{1}{c_l^{(n-1)}} (-\log(\hat{p}_l(\mathbf{c}^{(n-1)})))^{1/k}$

and for the modified Weibull form

$$c_l^{(n)} = \frac{1}{\tau_l^{(n)}} \left(\log \left(\frac{\gamma_l k c_l^{(n-1)^{k-1}} \tau_l^{(n)^k}}{\theta_l} \right) \right)^{1/k} \vee 1, \quad (38)$$

where in both cases

$$\gamma_l := \sum_{r \in \mathcal{R}} \lambda_r \sum_{i=1}^{N_r} \omega_{r,i} \prod_{j=1}^i (1_{l[l_j^{(r)}]} w_{r,j} + \bar{1}_l[l_j^{(r)}] (1 - \hat{p}_{r,j}(\mathbf{c}^{(n-1)}))).$$

By combining the update for c_l from (37) with the explicit solution for the τ_l from Table 2, Algorithm 3 for the ratio form can be viewed as fixed-point iteration of the mapping

$$H(\mathbf{c}) = \left(\frac{1}{\tau_l(\mathbf{c})} \left(-1 + \sqrt{\frac{\gamma_l k c_l^{k-1} \tau_l(\mathbf{c})^k}{\theta_l}} \right)^{1/k} \vee 1 \right)_{l \in \mathcal{L}},$$

where $\tau_l(\mathbf{c}) = \frac{1}{c_l^{(n-1)}} \left(\frac{1 - \hat{p}_l(\mathbf{c})}{\hat{p}_l(\mathbf{c})} \right)^{1/k}$. A similar characterisation can be obtain for the Weibull form. Assuming a maximum number of servers available to be allocated, the existence of a fixed point of H can be established using Brouwer's theorem.

In the next section we investigate the performance of the algorithm presented in this subsection, and compare it to Algorithm 2 (as presented in Section 4.2).

6. General Computational Experiments

In Section 4 and Section 5 we performed several computational experiments on various network instances, motivating our choice of functional forms and demonstrating the benefit of our approach. In this section

TABLE 3. Three combinations of rewards assigned to stations.

Revenue setting	Station 1	Station 2	Station 3	Station 4	Station 5	Station 6
Equal	1.25	1.25	1.25	1.25	1.25	1.25
Increasing	0.8	0.8	1.1	1.1	1.5	1.5
Unordered	1.25	1.1	0.8	1.5	3	1.1

we further investigate the performance of our algorithm on two larger scale and more complex systems. These examples are motivated by real-life systems and allow us to investigate high-dimensional instances of our approach.

6.1. Canonical networks. In this subsection we evaluate the performance of Algorithm 2 and Algorithm 3 on **Example 4** in Section 3.2. In all of the experiments the interarrival times and service times are generated from two-stage Coxian distributions with parameters set and scaled to match a collection of coefficients of variation (CoVs). We consider 100 randomly chosen (unique) scenarios where the interarrival times have a CoV randomly sampled from $\{0.75, 2, 3.25\}$, service times at stations 1 and 2 are randomly sampled from $\{2, 3.75, 5.5\}$, service times at stations 3 and 4 are randomly sampled from $\{1.5, 3, 4.5\}$, and service times at stations 5 and 6 are always equal to 1.5. The scenarios generated by this process are given in Table 6 in Appendix D.

The interarrival times for customers of class i are sampled as $\frac{1}{2\lambda_i}(E_1 + \frac{1}{q}E_2 B)$, where E_1 and E_2 are independent unit-mean exponentially distributed r.v.s, $q \in (0, 1)$ is a real number, and B is a Bernoulli r.v. with parameter q . The parameter $q = \frac{1}{2}v^{-2}$ is set s.t. CoV of the interarrival times matches the desired value v , specified in Table 6 for the scenario being studied. For classes $i = 1, \dots, 6$ we take $\lambda_i = 5$ and v equal to $A1$ as specified in the first column of Table 6. For classes $i = 1, \dots, 6$ we take $\lambda_i = 2.5$ and v equal to $A2$ as specified in the second column of Table 6. Service times are specified on a per-station basis. The service times of all customers at station i are sampled as $\frac{3}{8}(E_1 + \frac{1}{q}E_2 B)$, where E_1 , E_2 , B , and q are as before. For station i the CoV is set to match the value given in the $(2+i)$ -th column of Table 6. Capacity costs θ_i are assumed unitary for all stations. The amount of reward generated by a successful service $\omega_{r,i}$ is equal for all classes of customer at any particular station. We consider three different reward settings, as displayed in Table 3.

Our first goal is to understand how well the algorithms find an approximation to the optimal solution defined in (9). In order to find a benchmark we implemented a stochastic approximation algorithm (Algorithm 4 in Appendix B) for each scenario and reward setting. In Figure 6 we display the mean optimality gap from 10 sample paths of our Algorithm 2 and Algorithm 3 for the different scenarios and reward settings. It can be seen that both algorithms are capable of reliably achieving an optimality gap of less than 10% in most scenario and reward settings. In the equal reward setting both algorithms achieve an optimality gap of approximately 1%. In the increasing reward setting the performance is not quite as good and tends to be across the range 1–10% for both algorithms. In either of these reward settings it is positive to see that our algorithm which does not require access to a numerical optimisation package (Algorithm 3) does not lose accuracy compared to the algorithm which does have access to a numerical optimisation package (Algorithm 2). In fact, for the unordered weight setting Algorithm 3 has distinctly superior performance to Algorithm 2 in terms of accuracy.

Our second goal is to understand how efficient our algorithms are. Specifically, we would like to know how many iterations the algorithms require to reach a high level of accuracy. The average optimality

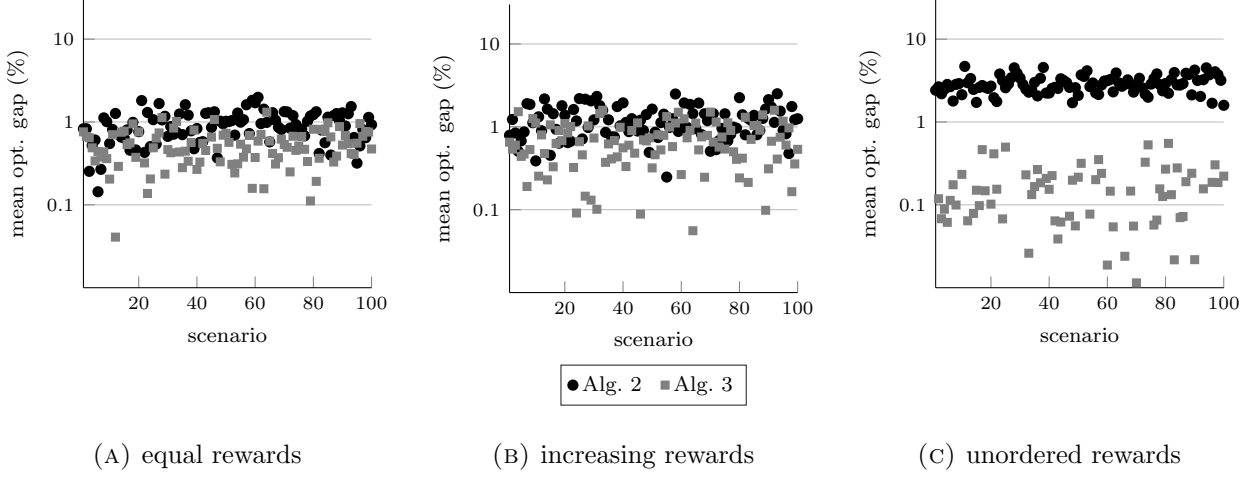


FIGURE 6. Accuracy of Algorithm 2 using form (b) with $k = 2$ and Algorithm 3 using form (d) with $k = 2$ for **Example 4** in Section 3.2 with the scenarios in Table 6.

gap at our randomly chosen initial conditions over the 3000 experiments we conducted was at least 55% (this is the average optimality gap considering only those experiments where the initial objective function value was positive) and in many cases exceeded 100%. In Figure 7 it can be seen that for all scenarios and reward settings where the optimality gap was reduced below 10%, this was always achieved in less than 5 iterations using Algorithm 3 and usually less than 5 iterations using Algorithm 2. To reduce the optimality gap below 1% the algorithms required approximately 10 iterations. Notably, since our method is derivative free it only requires a single sample of \hat{f} per iteration. In contrast, stochastic approximation with central finite-difference estimates (as in Algorithm 4) requires 12 samples of \hat{f} per iteration. The implication is that for many of the scenarios we considered in order to outperform our algorithm stochastic approximation would need to achieve an optimality gap of less than 1% in a single iteration.

6.2. Ring networks. In this subsection we consider a network consisting of a set of stations arranged in a ring. We consider a parameterisation of the model where some of the parameter values are randomly chosen as follows. For each of the stations we specify a Markov modulated Poisson process (MMPP) with three background states, according to which arrivals to the station occur. For all of these MMPPs, two of the background states result in customers arriving at rate 2 and the other results in customers arriving at a rate uniformly sampled from $(0, 4)$ (once for each MMPP). Each background chain jumps randomly between states at a rate which we sample uniformly from $(0, 1)$ (once for each MMPP). Upon jumping the background chain is equally likely to enter either of the other two states (other than the one it is jumping out of). Associated with arrivals at each station is a route over all other stations in the network. The costs of capacity at each station are sampled uniformly at random from $(0, 0.2)$ and stored in $\boldsymbol{\theta}$. The rewards for successfully processing customers are sampled uniformly at random from $(1, 2)$ on a per-route per-station basis and stored in $\boldsymbol{\omega}$.

Figure 8 compares sample paths of our algorithm ((b), (c), (e), and (f)) against stochastic approximation ((a) and (d)), as described in Appendix B, for this system with 10 stations (a) — (c) and 100 stations (d) — (e). We randomly chose five initial configurations and ran the optimisation algorithms. The figure shows that our approach achieves values comparable to stochastic approximation with fewer iterations. Due to the large number of samples needed per step the stochastic approximation sample paths took

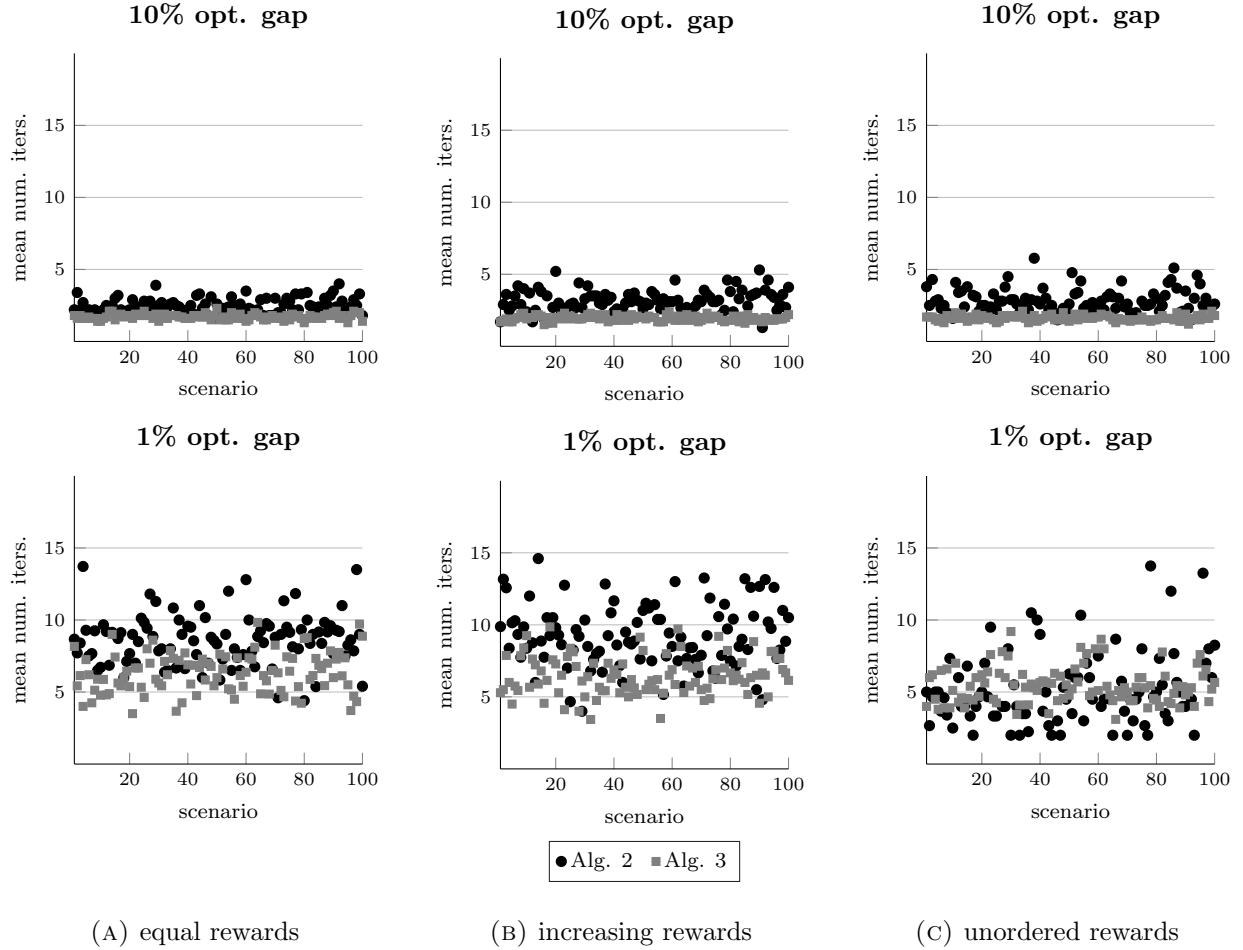


FIGURE 7. Efficiency of Algorithm 2 using form (b) with $k = 2$ and Algorithm 3 using form (d) with $k = 2$ for **Example 4** in Section 3.2 with the scenarios in Table 6.

vastly longer to generate than the functional form approach sample paths, with the 100 station example taking several days to complete in the case of stochastic approximation and all of the functional form sample paths completing in under an hour.

7. Conclusion

In this paper we considered the problem of optimising a stochastic network with blocking by allocating servers to each station in the network. Since increasing the number of servers comes at a cost, finding the optimal allocation requires finding a careful balance between network performance and service costs. We observed that existing approaches in the literature do not work because the network is too complex for analytical methods that rely on product-form approximations, and too large for existing computational approaches. We proposed a novel hybrid approach that combines analytical approximation of stochastic networks with simulation optimisation, and show that this approach significantly outperforms stochastic approximation in terms of the required computational effort.

Although we limited ourselves to stochastic networks with a particular type of blocking, our approach can be extended to more general networks, both with and without blocking. For instance, instead of considering a network where customers traverse a series of stations and may be blocked at any one of them, we could consider a network where customers are redirected to new stations until they find one

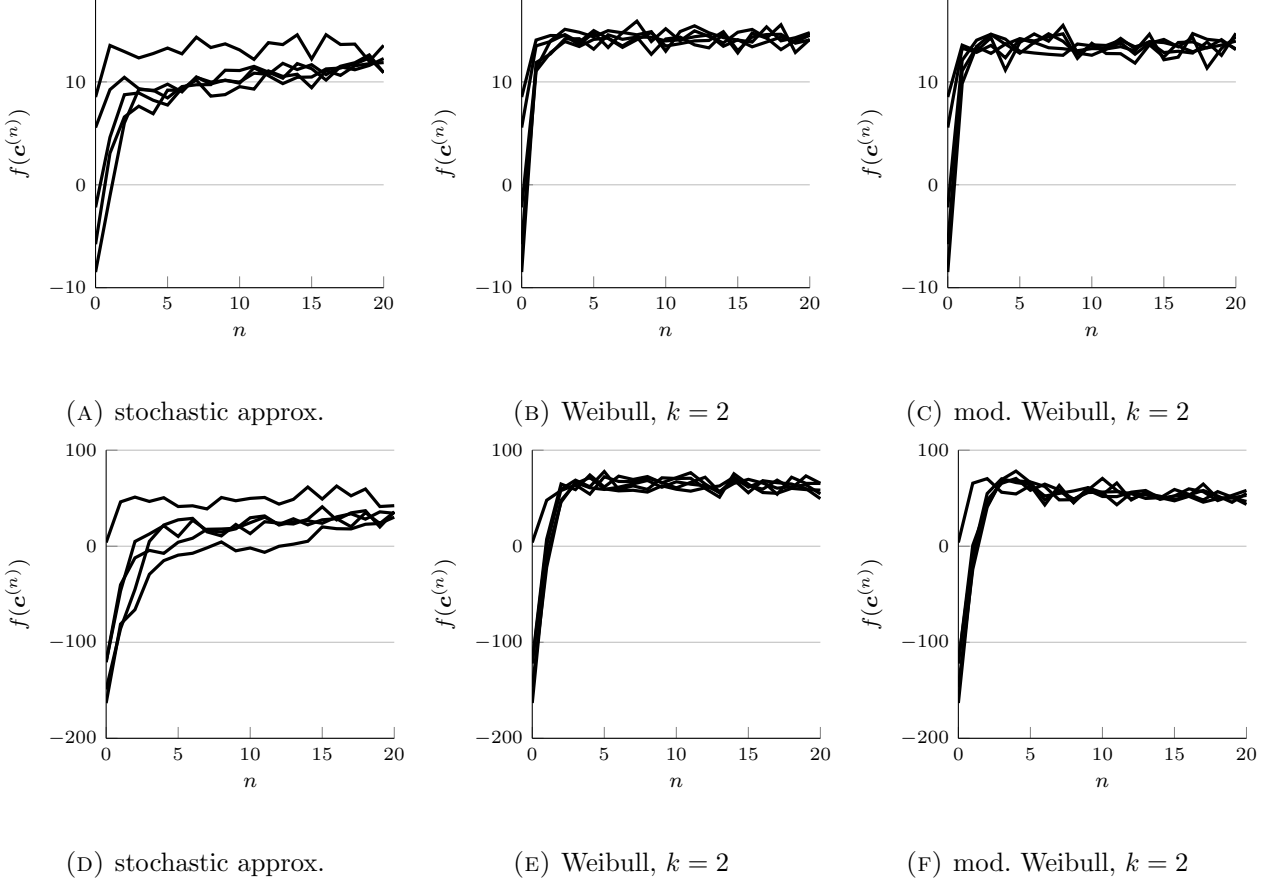


FIGURE 8. Sample paths for a ring network with 10 stations ((a) — (c)) or 100 stations ((d) — (e)) of stochastic approximation ((a) and (d)) and our algorithm with the Weibull form ((b) and (e)) and modified Weibull form ((c) and (f)).

with sufficient capacity. This corresponds for instance to a multi-echelon spare-part network, where a customer represent a request for the closest spare part. In order to extend our approach to this and other settings, new functional-form approximations need to be formulated and tested.

References

- [1] AberdeenGroup. Service parts management, unlocking value and profits in the service chain. *AberdeenGroup Boston*, 2003.
- [2] Prathima Agrawal, Dinesh K Anvekar, and Balakrishnan Narendran. Channel management policies for handovers in cellular networks. *Bell Labs Technical Journal*, 1(2):97–110, 1996.
- [3] Søren Asmussen and Peter W Glynn. *Stochastic simulation: algorithms and analysis*, volume 57. Springer Science & Business Media, 2007.
- [4] Sven Axsäter. Modelling emergency lateral transshipments in inventory systems. *Management Science*, 36(11):1329–1338, 1990.
- [5] Forest Baskett, K Mani Chandy, Richard R Muntz, and Fernando G Palacios. Open, closed, and mixed networks of queues with different classes of customers. *Journal of the ACM*, 22(2):248–260, 1975.
- [6] Sem C Borst, Avi Mandelbaum, and Martin I Reiman. Dimensioning large call centers. *Operations research*, 52(1):17–34, 2004.
- [7] Luce Brotcorne, Gilbert Laporte, and Frederic Semet. Ambulance location and relocation models. *European journal of operational research*, 147(3):451–463, 2003.

- [8] M. Brown and H. Solomon. A second-order approximation for the variance of a renewal reward process. *Stochastic Processes and their Applications*, 3:301–314, 1975.
- [9] Richard H Byrd, Samantha L Hansen, Jorge Nocedal, and Yoram Singer. A stochastic quasi-newton method for large-scale optimization. *SIAM Journal on Optimization*, 26(2):1008–1031, 2016.
- [10] Belinda A Chiera, Anthony E Krzesinski, and Peter G Taylor. Some properties of the capacity value function. *SIAM Journal on Applied Mathematics*, 65(4):1407–1419, 2005.
- [11] Belinda A Chiera and Peter G Taylor. What is a unit of capacity worth? *Probability in the Engineering and Informational Sciences*, 16(4):513–522, 2002.
- [12] Ton B Dieker, Soumyadip Ghosh, and Mark S Squillante. Optimal resource capacity management for stochastic networks. *Operations Research*, 65(1):221–241, 2017.
- [13] Arie Harel. Convexity properties of the erlang loss formula. *Operations Research*, 38(3):499–505, 1990.
- [14] J Michael Harrison and Ruth J Williams. Brownian models of feedforward queueing networks: Quasireversibility and product form solutions. *The Annals of Applied Probability*, pages 263–293, 1992.
- [15] J Michael Harrison and Assaf Zeevi. A method for staffing large call centers based on stochastic fluid models. *Manufacturing & Service Operations Management*, 7(1):20–36, 2005.
- [16] Refael Hassin, Yair Y Shaki, and Uri Yovel. Optimal service-capacity allocation in a loss system. *Naval Research Logistics (NRL)*, 62(2):81–97, 2015.
- [17] Q. He. *Fundamentals of Matrix-Analytic Methods*. Springer, New York, 2014.
- [18] Shane G Henderson and Barry L Nelson. *Handbooks in operations research and management science: simulation*, volume 13. Elsevier, 2006.
- [19] David L Jagerman. Some properties of the erlang loss function. *Bell Labs Technical Journal*, 53(3):525–551, 1974.
- [20] A. J. E. M. Janssen, J. S. H. Van Leeuwaarden, and B. Zwart. Gaussian expansions and bounds for the poisson distribution applied to the erlang b formula. *Advances in Applied Probability*, 40(1):122–143, 2008.
- [21] Frank P Kelly. Loss networks. *The annals of applied probability*, 1(3):319–378, 1991.
- [22] Jack Kiefer, Jacob Wolfowitz, et al. Stochastic estimation of the maximum of a regression function. *The Annals of Mathematical Statistics*, 23(3):462–466, 1952.
- [23] Leonard Kleinrock. *Communication nets: Stochastic message flow and delay*. McGraw–Hill, 1964.
- [24] Bram Kranenburg and Geert-Jan Van Houtum. A new partial pooling structure for spare parts networks. *European Journal of Operational Research*, 199(3):908–921, 2009.
- [25] Raymond Kwan, Rob Arnott, Robert Paterson, Riccardo Trivisonno, and Mitsuhiro Kubota. On mobility load balancing for LTE systems. In *Proceedings of IEEE Vehicular Technology Conference (VTC)*, 2010.
- [26] Yuyi Mao, Changsheng You, Jun Zhang, Kaibin Huang, and Khaled B Letaief. A survey on mobile edge computing: The communication perspective. *IEEE Communications Surveys & Tutorials*, 19(4):2322–2358, 2017.
- [27] S. Narayana and M. F. Neuts. The first two moment matrices of the counts for the Markovian arrival process. *Communications in statistics. Stochastic models*, 8(3):459–477, 1992.
- [28] B. Patch, Y. Nazarathy, and T. Taimre. A correction term for the covariance of renewal-reward processes with multivariate rewards. *Statistics & Probability Letters*, 102:1–7, 2015.
- [29] B. Patch and T. Taimre. Transient provisioning and performance evaluation for cloud computing platforms: A capacity value approach. *Performance Evaluation*, 118:48–62, 2018.
- [30] E. Pinsky. A simple approximation for the erlang loss function. *Performance evaluation*, 15(3):155–161, 1992.
- [31] S Rahimi-Ghahroodi, A Al Hanbali, WHM Zijm, JKW van Ommeren, and A Sleptchenko. Integrated planning of spare parts and service engineers with partial backlogging. *OR Spectrum*, pages 1–38, 2017.
- [32] Mateo Restrepo, Shane G Henderson, and Huseyin Topaloglu. Erlang loss models for the static deployment of ambulances. *Health care management science*, 12(1):67, 2009.
- [33] H. Robbins and S. Monro. A stochastic approximation method. In *Herbert Robbins Selected Papers*, pages 102–109. Springer, 1985.
- [34] Jaron Sanders, Sem C Borst, and Johan SH van Leeuwaarden. Online network optimization using product-form markov processes. *IEEE Transactions on Automatic Control*, 61(7):1838–1853, 2016.
- [35] Zuo-Jun Max Shen, Collette Coullard, and Mark S Daskin. A joint location-inventory model. *Transportation science*, 37(1):40–55, 2003.

- [36] Moshe Sidi and David Starobinski. New call blocking versus handoff blocking in cellular networks. *Wireless networks*, 3(1):15–27, 1997.
- [37] Pieter L Van den Berg, Guido AG Legemaate, and Rob D van der Mei. Increasing the responsiveness of firefighter services by relocating base stations in amsterdam. *Interfaces*, 47(4):352–361, 2017.
- [38] Pieter L Van den Berg, J Theresia van Essen, and Eline J Harderwijk. Comparison of static ambulance location models. In *Proceedings of Logistics Operations Management (GOL)*. IEEE, 2016.
- [39] Lawrence M Wein. Capacity allocation in generalized jackson networks. *Operations Research Letters*, 8(3):143–146, 1989.

Appendix A. Matrix Derivations

Although evaluation of the objective function in **Example 1** of Section 3.2 has been possible for quite some time using known methods, the power of the approach described in [29], based on matrix analytic methods (MAMs), is that far more general systems can be considered. **Example 3** in Section 3.2 is such a system. This section uses these methods to explicitly compute our objective for this example, so that it can be used to exactly test our simulation method.

MAMs for Example 3. Here we explain how to obtain explicit expressions for each of the reward terms in (13), i.e., for

$$\begin{aligned}\kappa_1 &:= \lambda_1 \omega_{1,1} (1 - p_{1,1}(c_1)), \\ \kappa_2 &:= \lambda_1 \omega_{1,2} (1 - p_{1,1}(c_1))(1 - p_{1,2}(c)),\end{aligned}$$

using matrix analytic methods.

Let $X_{1,1}(t)$ and $X_{1,2}(t)$ be the number of customers being processed by the system at the first and second stations respectively. Following [29], we observe that this description leads to a marked MAP (see, e.g. [17, Section 2.5] for details), $(N_1(t), N_2(t), t \in \mathbb{R}_0)$, that counts the number of customers successfully entering the first and second stations as follows. Upon an arrival to the first station, as long as $X_{1,1} < c_1$, then $X_{1,1}$ jumps up by 1 and so does N_1 . Upon a successful service completion at the first station, if $X_{1,2} < c_2$ then $X_{1,2}$ jumps up by 1 and so too does N_2 . It can be seen that the process $(X_{1,2}, X_{1,2})$ is a background process for an encompassing MAP that experiences arrivals when customers enter stations. In order to find κ_1 and κ_2 explicitly we need to carefully construct the structure of the Markov chain $(X_{1,1}, X_{1,2})$, specify its relationship to N_1 and N_2 , and then apply Theorem 1 from [27].

In order to obtain expressions for κ_1 and κ_2 we need to define several matrices. Let:

- $\mathbf{1}_k$ be a k -tuple containing all unit entries.
- I_k be a $k \times k$ identity matrix.
- \bar{I}_k be a $k \times k$ matrix with upper diagonal containing unit entries and otherwise 0.
- \underline{I}_k be a $k \times k$ matrix with lower diagonal containing unit entries and otherwise 0.
- Q_1 be a $(c_1 + 1) \times (c_1 + 1)$ matrix with non-zero entries

$$\begin{aligned}(Q_1)_{i,i+1} &= \lambda_1, & \text{for } i = 1, \dots, c_1, \\ (Q_1)_{i+1,i} &= (i+1)\mu_1, & \text{for } i = 1, \dots, c_1, \\ (Q_1)_{i,i} &= -(\lambda_1 + (i-1)\mu_1), & \text{for } i = 1, \dots, c_1, \\ (Q_1)_{c_1+1,c_1+1} &= -c_1\mu_1.\end{aligned}$$

- Q_2 be a $(c_2 + 1) \times (c_2 + 1)$ matrix with non-zero entries

$$\begin{aligned}(Q_2)_{i,i+1} &= \lambda_2, & \text{for } i = 1, \dots, c_2, \\ (Q_2)_{i+1,i} &= (i+1)\mu_2, & \text{for } i = 1, \dots, c_2, \\ (Q_2)_{i,i} &= -(\lambda_2 + (i-1)\mu_2), & \text{for } i = 1, \dots, c_2, \\ (Q_2)_{c_2+1,c_2+1} &= -c_2\mu_2.\end{aligned}$$

- \bar{Q}_1 be a $(c_1 + 1) \times (c_1 + 1)$ matrix with non-zero entries

$$(Q_1)_{i,i} = -(i-1)\mu_1, \quad \text{for } i = 1, \dots, c_1.$$

- \bar{Q}_2 be a $(c_2 + 1) \times (c_2 + 1)$ matrix with non-zero entries

$$(Q_2)_{i,i} = -(i-1)\mu_2, \quad \text{for } i = 1, \dots, c_2.$$

Then, use these to define

$$\begin{aligned} D &= (I_{c_2+1} \otimes Q_1) + (Q_2 \otimes I_{c_1+1}), \\ D_{1,1} &= \bar{I}_{c_2+1} \otimes \bar{Q}_1, \\ D_{1,2} &= \bar{Q}_2 \otimes \underline{I}_{c_1+1}. \end{aligned}$$

Take π to be the stationary distribution of the Markov chain generated by infinitesimal generator D , i.e., $\pi D = 0$ and $\pi \mathbf{1}_{(c_1+1)(c_2+1)} = 1$. We then obtain the following expression for the expected number of successfully processed customers at each station using [27, Theorem 1]:

$$\begin{aligned} \mathbb{E} N_1(t) &= \pi D_{1,1} \mathbf{1}_{(c_1+1)(c_2+1)} t + o(t), \\ \mathbb{E} N_2(t) &= \pi D_{1,2} \mathbf{1}_{(c_1+1)(c_2+1)} t + o(t), \end{aligned}$$

where $o(t) \rightarrow 0$ is a function $h(t)$ s.t. $h(t)/t \rightarrow 0$ as $t \rightarrow \infty$. The quantities of interest κ_1 and κ_2 follow immediately from differentiation of this expression and multiplication by the appropriate θ term. Based on this we can explicitly compute (13) for our tandem network of loss systems.

Appendix B. Stochastic Approximation Implementation

For $\mathcal{C} \subset \mathbb{R}^d$, let $\Pi_{\mathcal{C}}$ be a function $\mathbb{R}^d \rightarrow \mathcal{C}$ that, for $\mathbf{x} \in \mathbb{R}^d$, returns $\mathbf{c} \in \mathcal{C}$ which minimises $\|\mathbf{c} - \mathbf{x}\|$. Let \mathbf{e}_l be a vector with all components 0 except for component l , which is unitary, and let $\{\delta^{(n)}\}_{n \in \mathbb{N}}$ and $\{\alpha^{(n)}\}_{n \in \mathbb{N}}$ be sequences satisfying

$$\sum_{n=1}^{\infty} \alpha^{(n)} = \infty, \quad \sum_{n=1}^{\infty} \alpha^{(n)} \delta^{(n)} < \infty, \quad \sum_{n=1}^{\infty} \alpha^{(n)2} \delta^{(n)-2} < \infty. \quad (39)$$

Then, if \widehat{f} are uniformly bounded r.v.s, Algorithm 4 is a convergent (in probability) stochastic approximation algorithm [22].

Algorithm 4: Stochastic approximation.

Result: Approximation to optimal capacity allocation.

- 1 Choose $\mathbf{c}^{(0)} \in (0, \infty)^L$, $\epsilon > 0$, $N \in \mathbb{N}$;
- 2 Set $n = 1$ and $g > \epsilon$;
- 3 **while** $g > \epsilon$ and $n \leq N$ **do**
- 4 Determine estimates $(\widehat{\nabla_{\mathbf{c}} f}(\mathbf{c}^{(n-1)}))_l = \frac{\widehat{f}(\mathbf{c}^{(n-1)} + \delta^{(n)} \mathbf{e}_l) - \widehat{f}(\mathbf{c}^{(n-1)} - \delta^{(n)} \mathbf{e}_l)}{2\delta^{(n)}}$ for components $l = 1, \dots, L$ of the Jacobian;
- 5 Choose a step size $\alpha^{(n)}$;
- 6 Set $\mathbf{c}^{(n)} = \Pi_{\mathcal{C}}(\mathbf{c}^{(n-1)} + \alpha^{(n)} \widehat{\nabla_{\mathbf{c}} f}(\mathbf{c}^{(n-1)}))$;
- 7 Set $g = \|\mathbf{c}^{(n-1)} - \mathbf{c}^{(n)}\|$ and $n = n + 1$;
- 8 **end**
- 9 Output $\mathbf{c}^{(n)}$.

In each iteration of this algorithm the step size $\alpha^{(n)}$ can be determined using the following backtracking line-search method. First choose $\beta > 0$, $\varrho_1 \in (0, 1)$, $\varrho_2 \in (0, 1)$, $D > 0$. Set $\alpha^{(n)} = \beta^{(n)}$ and $d = 1$, and then:

- (I) Determine $F = \widehat{f}\left(\Pi_{\mathcal{C}}\left(\mathbf{c}^{(n-1)} + \alpha^{(n)} \widehat{\nabla_{\mathbf{c}} f}(\mathbf{c}^{(n-1)})\right)\right)$.
- (II) If $F \geq \widehat{f}(\mathbf{c}^{(n-1)}) + \varrho_2 \alpha^{(n)} \widehat{\nabla_{\mathbf{c}} f}(\mathbf{c}^{(n-1)})$ or $d \geq D$: output $\alpha^{(n)}$.
Else: set $\alpha^{(n)} = \varrho_1 \alpha^{(n)}$ and $d = d + 1$, and return to (I).

Choosing $\beta^{(n)} = \beta n^{-1/3}$ where $\beta \in \mathbb{R}_+$ is a positive real number and $\delta^{(n)} = n^{-1/6}$ ensures that (39) holds and the algorithm therefore converges to the true optimiser with probability 1.

Appendix C. Evidence supporting enhanced functional form

Each of the following subsections provides computational or simulation based evidence to support the modifications to the functional form presented in Section 4 performed in a corresponding subsection of Section 5.

C.1. Single-station case. Figure 9 plots the progression of Algorithm 2 for the single-station case using the modified forms (c) and (d) in comparison with the corresponding cases using (a) and (b) (with the same parameter settings as used in Figure 4, but with an initial condition $c_1^{(0)} = 30$). It can be seen that the modified form sample paths track the sample paths of the unmodified forms very closely.

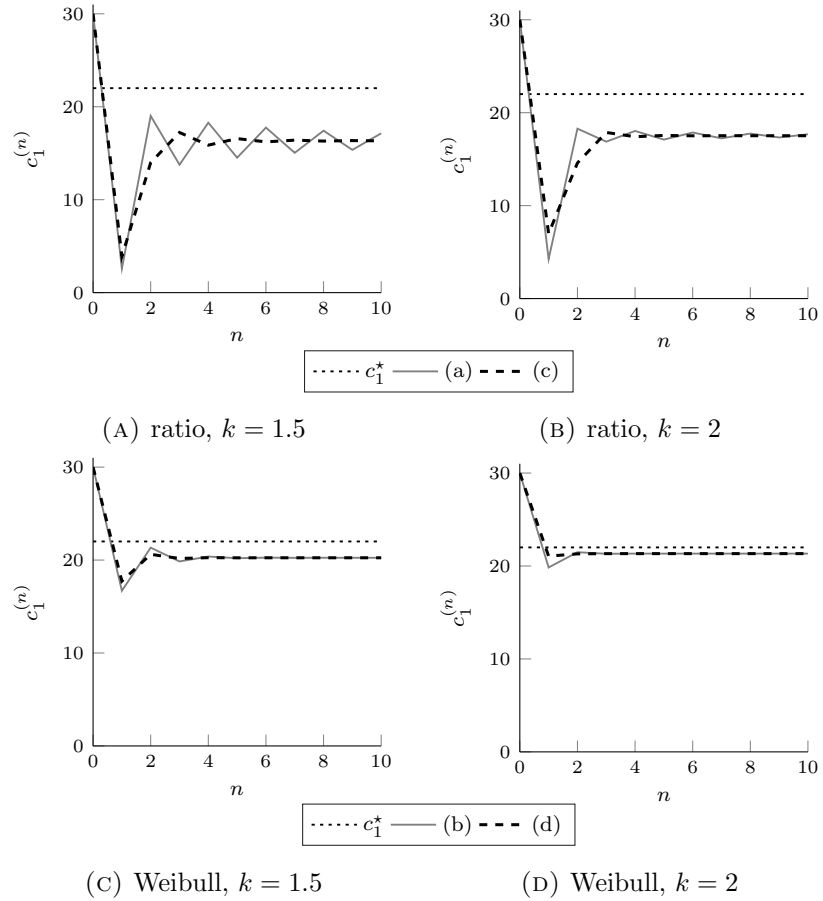


FIGURE 9. Comparison of evolution of Algorithm 1 with different forms.

C.2. Tandem networks. As a representative example, for an arrival rate $\lambda_1 = 16$, capacity cost $\theta_1 = 0.2$ and $\theta_2 = 0.3$, and reward $\omega_{1,1} = \omega_{1,2} = 1$, computations from the MAM approach provide the true maximum of $f(\mathbf{c}^*) = 20.4262$ over the objective function (13). In comparison, Table 4 presents the solutions attained by Algorithm 2 using a numerical solver and using (29) and (30) across different choices of k . For each of 100 randomly chosen initial conditions, we generate a sample path for each functional form with varying choices of $k = 1, \dots, 10$. Table 4 reports for each functional form and each k the mean and variance of the objective function value evaluated at the capacity allocation from Algorithm 2 over the 100 sample paths together with the mean number of iterations before the stopping condition $|c_1^{(n)} - c_1^{(n-1)}| + |c_2^{(n)} - c_2^{(n-1)}| < \epsilon = 1$ or $n = N := 20$ is reached.

TABLE 4. Objective function from Algorithm 2 using a numerical solver and using explicit solutions applied to **Example 3** of Section 3.2. Each entry provides the mean and variance of the objective function value at the capacity given by the final iteration over 100 sample paths, each generated with a unique $\mathbf{c}^{(0)} \in \mathbb{Z}^2 \cap [1, 100]^2$. The true optimal value is **20.4262**.

k	Mean obj. val.	Var obj. val.	Mean no. of iter.	Mean obj. val.	Var obj. val.	Mean no. of iter.	
Algorithm 2				Algorithm 2 using (29) and (30)			
(a) Ratio				(c) Modified ratio			
1	12.4302	1.1868	20.0000	12.3515	1.3464	20.0000	
2	16.1691	7.3017	19.2800	19.7043	0.0492	11.3000	
3	19.7975	0.4250	16.1600	20.0526	0.0178	7.4400	
4	20.1324	0.0677	14.3800	20.1560	0.0148	6.0800	
5	20.1969	0.0303	12.2700	20.2234	0.0137	6.5300	
6	20.1320	0.3671	10.5400	20.2274	0.0112	5.4500	
7	20.2012	0.0187	9.9500	20.2443	0.0090	5.9000	
8	20.1999	0.0149	9.6500	20.2319	0.0075	5.5400	
9	20.1804	0.0152	8.9000	20.1988	0.0116	5.3400	
10	20.1164	0.0271	9.4900	20.1427	0.1463	5.5400	
(b) Weibull				(d) Modified Weibull			
1	19.5870	0.3936	15.5200	19.5206	0.7876	17.3600	
2	20.1473	0.0128	9.2400	20.1658	0.0154	7.8800	
3	20.0670	0.0294	8.5000	20.0692	0.0204	6.9200	
4	19.9180	0.0373	7.6400	19.9556	0.0485	6.8100	
5	19.7887	0.0403	7.7000	19.7673	0.0593	8.1100	
6	19.7043	0.0756	7.7800	19.6591	0.0654	8.6200	
7	19.5371	0.1212	8.6700	19.5080	0.0994	9.9400	
8	19.4220	0.1018	9.2700	19.3588	0.1874	10.4000	
9	19.3057	0.1370	10.7200	19.3022	0.2251	12.6800	
10	19.2221	0.2935	11.5900	19.1025	0.3602	13.3000	

We observe from this example that the ratio and Weibull forms continue to perform quite well. Importantly, our modified forms do not display reduced accuracy in comparison with their original counterparts, and in some cases are in fact more accurate. The modifications for the ratio form case yield a noticeable reduction in the number of iterations needed to achieve convergence, while the number of iterations needed for convergence of the Weibull form case do not appear to be substantially affected by the modifications.

To study the accuracy and efficiency of our modified functional forms in more general tandem networks, we compare performance over 100 different scenarios. Each of these scenarios has rewards chosen uniformly at random from the interval $(0, 2)$, mean service times chosen uniformly at random from the interval $(1/3, 1)$, arrival rate chosen uniformly at random from the interval $(10, 20)$, first-station cost chosen uniformly at random from the interval $(0.1, 0.3)$, and second-station cost chosen uniformly at random from the interval $(0.1, 0.4)$. To ensure the MAM-based computations to find the true optimiser are not too burdensome, we only experimented with scenarios where the true optimum was within $(1, 30)^2$. Upon

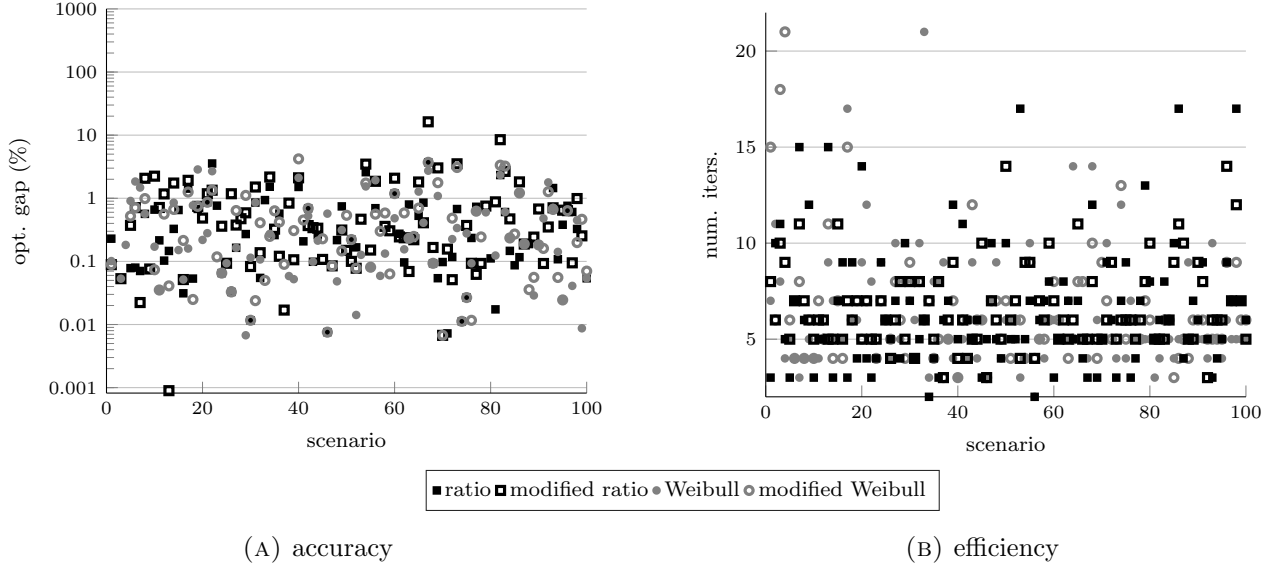


FIGURE 10. Comparison of two-station tandem network performance for ratio ($k = 7$), modified ratio ($k = 8$), Weibull ($k = 2$), and modified Weibull ($k = 2$) forms over a variety of scenarios.

generating 100 suitable scenarios, we used each to compute a sample path of our algorithm for the ratio ($k = 7$), modified ratio ($k = 8$), Weibull ($k = 2$), and modified Weibull ($k = 2$) functional forms. The initial condition for each scenario was chosen uniformly at random from $(1, \dots, 100)^2$ and held constant across the different forms. The choices of k reflect values that performed well in the experiments used to generate Table 4.

To investigate the accuracy of our algorithm, Figure 10a reports the optimality gap achieved by our algorithm under the various functional forms, relative to the exact optimal value with the same stopping condition used in Table 4. For many cases it can be observed that our algorithms achieve an optimality gap of less than 1%, with only one instance exhibiting an optimality gap of greater than 10%. To investigate the efficiency of our algorithm, Figure 10b reports the number of iterations needed to obtain the optimality gap reported in Figure 10a. It can be observed that the bulk of the experiments required a number of iterations less than 10, indeed many required approximately 5 iterations, and very few required more than 15 iterations.

C.3. Two customer classes. This subsection presents some results that allow us to investigate the effectiveness of the modification to our approach detailed in Subsection 5.3. For the single-station, two-class system, customers of class $i \in \{1, 2\}$ arrive according to a renewal process with i.i.d. two-stage Coxian distributed interarrival times sampled as $\frac{1}{2\lambda_i}(E_1 + \frac{1}{q_i}E_2 B)$, where E_1 and E_2 are independent unit-mean exponentially distributed r.v.s, $q \in (0, 1)$ is a real number, and B is a Bernoulli r.v. with expected value q_i . The parameter $q_i = \frac{1}{2}v_i^{-2}$ is set s.t. the coefficient of variation (CoV) matches a chosen value. We set $\lambda_1 = 12$, $\lambda_2 = 20$, noting that this set-up means that these parameters are also the long term average arrival rates as defined in (6). We choose q s.t. the CoV is 0.75 for class 1 customers and 1.25 for class 2 customers. We suppose that successfully serving a class 1 customer renders a reward of $\omega_{1,1} = 0.8$, and successfully serving a class 2 customer renders a reward of $\omega_{2,1} = 1.2$. The capacity cost is set to $\theta = 0.3$, and service times follow a unit-mean exponential distribution.

TABLE 5. Objective function from Algorithm 2 using a numerical solver and using explicit solutions applied to **Example 2** of Section 3.2. Each entry provides the mean and variance of the objective function value at the capacity given by the final iteration over 100 sample paths, each generated with a unique $\mathbf{c}^{(0)} \in \mathbb{Z}^2 \cap [1, 100]^2$. The optimal value from stochastic approximation is approximately **21.7773**.

k	Mean obj. val.	Var obj. val.	Mean no. of iter.	Mean obj. val.	Var obj. val.	Mean no. of iter.	
Algorithm 2				Algorithm 2 using (29) and (30)			
(a) Ratio				(c) Modified ratio			
1	16.0822	0.2917	5.0400	16.2271	0.3113	5.2700	
2	19.2738	0.4277	9.8400	19.2778	0.5086	4.0200	
3	20.1238	0.5094	7.6700	20.0334	0.4319	3.6000	
4	20.5314	0.4616	5.0300	20.4403	0.3577	3.8000	
5	20.7231	0.2731	4.2500	20.6639	0.2414	3.5900	
6	20.7009	0.2757	3.9800	20.7316	0.2364	3.5500	
7	20.7269	0.2345	4.2800	20.6271	4.0171	3.3500	
8	20.7974	0.2221	3.7900	20.5411	3.9306	3.5800	
9	20.7680	0.1786	3.9400	20.4959	3.9669	3.7600	
10	20.7576	0.1717	4.1100	20.4048	7.7001	4.2700	
(b) Weibull				(d) Modified Weibull			
1	19.5939	0.4274	7.8700	19.6470	0.4723	6.9300	
2	20.7438	0.2294	3.1400	20.7697	0.2218	3.1800	
3	20.8009	0.1641	3.1600	20.7749	0.1862	3.1300	
4	20.6955	0.1322	3.7500	20.6699	0.1416	3.8400	
5	20.5658	0.1396	4.1800	20.6030	0.1010	4.7700	
6	20.5741	0.1565	4.6300	20.5343	0.1584	5.3200	
7	20.4319	0.1566	4.6600	20.1516	3.8280	4.9600	
8	20.3487	0.1776	4.8900	20.0492	3.7379	5.3100	
9	20.0617	3.7768	5.2600	19.9491	3.9616	6.1300	
10	19.7322	7.2169	6.2200	19.5571	10.5168	7.0000	

We applied stochastic approximation (Algorithm 4 in Appendix B) to this system several times with different initial conditions to obtain a benchmark of 21.7773 for the optimal performance. We sampled 100 unique initial conditions and then ran our algorithm with these initial conditions using each functional form with various values of k . The corresponding mean and variance of the objective function values, together with the mean number of iterations for these values, are presented in Table 5. It can be observed that the ratio and Weibull forms, which worked well for the simple Erlang system and the tandem system, continue to work well in this setting. Of primary importance, however, is that we again see that our modified forms perform comparably to our original forms. Interestingly, higher values of k now appear to result in more variance in the optimal value obtained by the algorithm. For this reason, we proceed in further experiments with $k = 8$ for the ratio form, $k = 6$ for the modified ratio form, and $k = 2$ for the Weibull and modified Weibull forms.

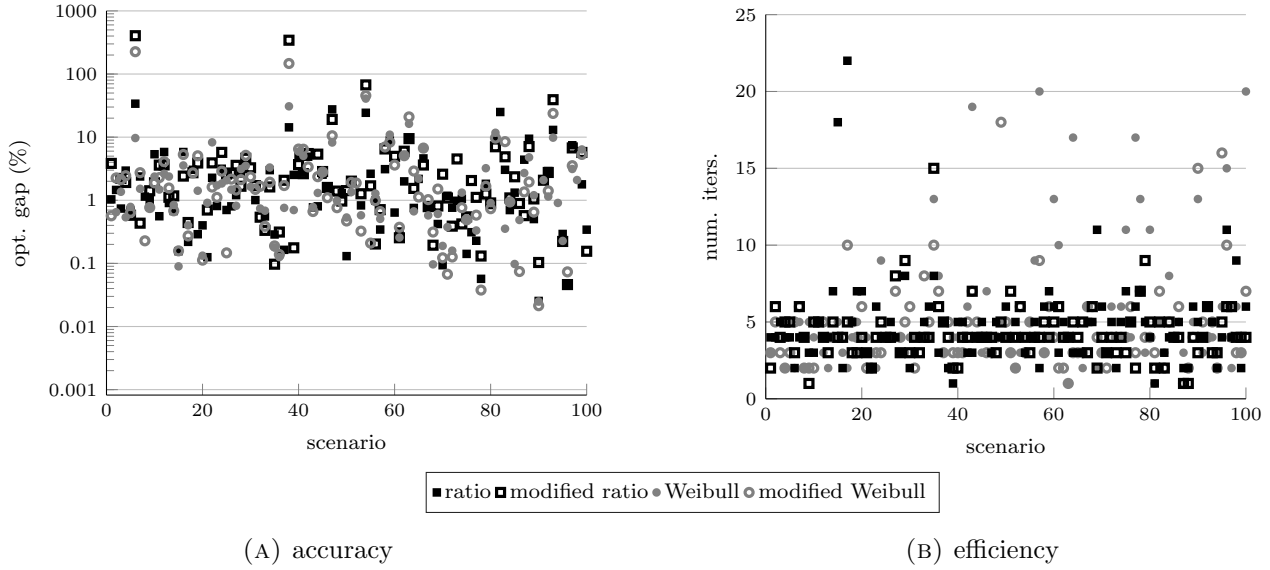


FIGURE 11. Comparison of single-station, two-class network performance for ratio ($k = 8$), modified ratio ($k = 6$), Weibull ($k = 2$), and modified Weibull ($k = 2$) forms over a variety of scenarios.

Finally, Figure 11 provides evidence that the modification presented in this subsection does not degrade our algorithm performance across various parameter settings for the system used to generate Table 5. Similar to the previous subsection, we randomly generated 100 different scenarios and report on accuracy and efficiency. In these experiments we selected λ_1 uniformly from $(4, 9)$, λ_2 uniformly from $(8, 18)$, CoVs uniformly from $(1, 2)$, service times according to an exponential distribution with mean selected uniformly from $(\frac{2}{3}, 2)$. For many of the scenarios an optimality gap of less than 1% is achieved, and only approximately 3% of the scenarios had an optimality gap of greater than 10%. (In a small number of cases our algorithm achieved a final estimated objective function value slightly better than stochastic approximation, but these are not displayed in the figure and likely due to noise.) This performance occurs in many cases from less than 5 iterations; in only a small number of cases are more than 10 iterations required; and the greatest number of iterations was never more than approximately 20. We continue to observe that our modified forms provide comparable accuracy and efficiency to the originally proposed forms.

Appendix D. Simulation scenarios

TABLE 6. Coefficients of variation for the experiments in Section 6.1.

	$A1$	$A2$	$S1$	$S2$	$S3$	$S4$	$S5$	$S6$		$A1$	$A2$	$S1$	$S2$	$S3$	$S4$	$S5$	$S6$
1	4.5	4.5	2	2	0.75	0.75	1.5	1.5	51	0.75	3.25	3.75	3.75	4.5	3	1.5	1.5
2	3	4.5	2	2	3.25	0.75	1.5	1.5	52	0.75	3.25	3.75	3.75	4.5	4.5	1.5	1.5
3	4.5	3	2	2	3.25	0.75	1.5	1.5	53	2	3.25	3.75	3.75	3	4.5	1.5	1.5
4	4.5	4.5	2	2	3.25	0.75	1.5	1.5	54	3.25	3.25	3.75	3.75	1.5	4.5	1.5	1.5
5	4.5	1.5	2	2	0.75	2	1.5	1.5	55	3.25	3.25	3.75	3.75	3	3	1.5	1.5
6	3	1.5	2	2	2	2	1.5	1.5	56	0.75	0.75	5.5	3.75	4.5	4.5	1.5	1.5
7	1.5	3	2	2	0.75	3.25	1.5	1.5	57	2	0.75	5.5	3.75	1.5	1.5	1.5	1.5
8	1.5	4.5	2	2	0.75	3.25	1.5	1.5	58	3.25	0.75	5.5	3.75	3	1.5	1.5	1.5
9	4.5	3	2	2	0.75	3.25	1.5	1.5	59	0.75	2	5.5	3.75	4.5	1.5	1.5	1.5
10	4.5	3	2	2	2	3.25	1.5	1.5	60	2	2	5.5	3.75	4.5	4.5	1.5	1.5
11	3	4.5	3.75	2	0.75	0.75	1.5	1.5	61	2	3.25	5.5	3.75	3	1.5	1.5	1.5
12	3	3	3.75	2	2	0.75	1.5	1.5	62	2	3.25	5.5	3.75	4.5	4.5	1.5	1.5
13	1.5	4.5	3.75	2	3.25	0.75	1.5	1.5	63	3.25	3.25	5.5	3.75	1.5	1.5	1.5	1.5
14	3	3	3.75	2	3.25	0.75	1.5	1.5	64	3.25	3.25	5.5	3.75	1.5	3	1.5	1.5
15	1.5	1.5	3.75	2	0.75	2	1.5	1.5	65	0.75	0.75	2	5.5	4.5	4.5	1.5	1.5
16	3	1.5	3.75	2	0.75	2	1.5	1.5	66	2	0.75	2	5.5	1.5	1.5	1.5	1.5
17	4.5	1.5	3.75	2	0.75	2	1.5	1.5	67	2	0.75	2	5.5	4.5	3	1.5	1.5
18	1.5	3	3.75	2	2	2	1.5	1.5	68	3.25	0.75	2	5.5	1.5	4.5	1.5	1.5
19	3	1.5	3.75	2	2	2	1.5	1.5	69	3.25	0.75	2	5.5	3	4.5	1.5	1.5
20	4.5	3	3.75	2	2	2	1.5	1.5	70	0.75	2	2	5.5	1.5	3	1.5	1.5
21	1.5	3	3.75	2	0.75	3.25	1.5	1.5	71	0.75	2	2	5.5	3	3	1.5	1.5
22	4.5	4.5	3.75	2	0.75	3.25	1.5	1.5	72	0.75	3.25	2	5.5	1.5	3	1.5	1.5
23	1.5	3	5.5	2	0.75	0.75	1.5	1.5	73	0.75	3.25	2	5.5	3	4.5	1.5	1.5
24	3	3	5.5	2	0.75	0.75	1.5	1.5	74	0.75	3.25	2	5.5	4.5	3	1.5	1.5
25	4.5	1.5	5.5	2	2	0.75	1.5	1.5	75	2	3.25	2	5.5	1.5	1.5	1.5	1.5
26	3	1.5	5.5	2	3.25	0.75	1.5	1.5	76	2	3.25	2	5.5	1.5	3	1.5	1.5
27	3	4.5	5.5	2	3.25	0.75	1.5	1.5	77	2	3.25	2	5.5	1.5	4.5	1.5	1.5
28	4.5	3	5.5	2	3.25	0.75	1.5	1.5	78	2	3.25	2	5.5	3	1.5	1.5	1.5
29	1.5	4.5	5.5	2	0.75	2	1.5	1.5	79	3.25	3.25	2	5.5	1.5	1.5	1.5	1.5
30	3	1.5	5.5	2	2	2	1.5	1.5	80	0.75	0.75	3.75	5.5	1.5	3	1.5	1.5
31	1.5	3	5.5	2	3.25	2	1.5	1.5	81	2	0.75	3.75	5.5	1.5	3	1.5	1.5
32	1.5	3	5.5	2	2	3.25	1.5	1.5	82	2	0.75	3.75	5.5	3	1.5	1.5	1.5
33	4.5	1.5	5.5	2	2	3.25	1.5	1.5	83	2	0.75	3.75	5.5	4.5	3	1.5	1.5
34	1.5	4.5	2	3.75	0.75	0.75	1.5	1.5	84	3.25	0.75	3.75	5.5	4.5	4.5	1.5	1.5
35	3	4.5	2	3.75	0.75	0.75	1.5	1.5	85	0.75	2	3.75	5.5	4.5	1.5	1.5	1.5
36	3	1.5	2	3.75	2	0.75	1.5	1.5	86	0.75	2	3.75	5.5	4.5	4.5	1.5	1.5
37	3	3	2	3.75	2	0.75	1.5	1.5	87	2	2	3.75	5.5	1.5	4.5	1.5	1.5
38	4.5	3	2	3.75	0.75	2	1.5	1.5	88	3.25	2	3.75	5.5	1.5	1.5	1.5	1.5
39	4.5	4.5	2	3.75	0.75	2	1.5	1.5	89	3.25	2	3.75	5.5	4.5	3	1.5	1.5
40	4.5	1.5	2	3.75	2	2	1.5	1.5	90	0.75	0.75	5.5	5.5	1.5	3	1.5	1.5
41	1.5	3	2	3.75	2	3.25	1.5	1.5	91	2	0.75	5.5	5.5	4.5	4.5	1.5	1.5
42	3	3	2	3.75	3.25	3.25	1.5	1.5	92	3.25	0.75	5.5	5.5	1.5	3	1.5	1.5
43	1.5	1.5	3.75	3.75	0.75	0.75	1.5	1.5	93	3.25	0.75	5.5	5.5	1.5	4.5	1.5	1.5
44	3	3	3.75	3.75	0.75	0.75	1.5	1.5	94	0.75	2	5.5	5.5	1.5	4.5	1.5	1.5
45	1.5	1.5	3.75	3.75	3.25	0.75	1.5	1.5	95	0.75	2	5.5	5.5	3	4.5	1.5	1.5
46	3	1.5	3.75	3.75	3.25	0.75	1.5	1.5	96	2	2	5.5	5.5	4.5	4.5	1.5	1.5
47	1.5	4.5	3.75	3.75	0.75	2	1.5	1.5	97	3.25	2	5.5	5.5	3	3	1.5	1.5
48	4.5	1.5	3.75	3.75	0.75	2	1.5	1.5	98	3.25	2	5.5	5.5	4.5	1.5	1.5	1.5
49	3	1.5	3.75	3.75	2	2	1.5	1.5	99	0.75	3.25	5.5	5.5	3	4.5	1.5	1.5
50	4.5	4.5	3.75	3.75	2	2	1.5	1.5	100	3.25	3.25	5.5	5.5	4.5	1.5	1.5	1.5